Final Report

Advanced Fuel Injector for a Catalytic Micro-Channel Fuel Cell Processor

December 2002

Prepared for:
Washington Technology Center
Seattle, Washington

Prepared by:
Philip C. Malte, Andrew Campbell Lee,
Andrew Chong Sung Lee, Igor Novosselov, and Stephen de Bruyn Kops
Energy and Environmental Combustion Laboratory
Department of Mechanical Engineering
University of Washington
Seattle, Washington 98195-2600

with
W. Lloyd Allen
InnovaTek, Inc.
350 Hills Street, Suite 104
Richland, Washington 99352

TABLE OF CONTENTS

TABLE OF CONTENTS CONTINUED

LIST OF TABLES

LIST OF FIGURES

LIST OF FIGURES CONTINUED

LIST OF FIGURES CONTINUED

LIST OF FIGURES CONTINUED

Advanced Fuel Injector for a Catalytic Micro-Channel Fuel Cell Processor

Summary

This study has involved the design and testing of an advanced injector for atomizing, vaporizing, and mixing diesel fuel into superheated steam without the detrimental effects of unmixedness and carbon formation on the internal components of the catalytic micro-channel reactor that produces hydrogen for fuel cell use.

The study was begun 1 January 2001 and concluded 30 September 2002 under 86% support from the Washington Technology Center and 14% support from InnovaTek, Inc.

The original plans specified design of an injector sized for a 100 watts fuel cell. However, during the project, InnovaTek requested the injector be resized for a fuel cell of 1000 watts power output.

The study, in chronological order, involved the following tasks:

1. *Injector concepts and design:* Preliminary examination of candidate injector concepts using CFD (computational fluid dynamics). The injector selected and designed for testing uses a jet of diesel fuel surrounded by steam passing through a small atomizing nozzle into the injector tube.

2. *Experimental rig:* Design, fabrication, assembly, and testing of the experimental rig, consisting of the steam generator, diesel fuel system, the injector, and instrumentation for the measurement of flow rate, temperature, and pressure. The original system was built for the 100 watt fuel cell, and then was modified for the 1000 watts fuel cell.

3. *Injector testing:* Testing was conducted on the injector sized for the 1000 watts fuel cell. Nominal injector pressure was 70 psig, meeting the design specification. Maximum steam temperature was 550 degrees C. The nominal ratio of steam to diesel mass flow was 4. Heat absorbed by the diesel fuel undergoing vaporization caused the diesel-steam mixture temperature in the injector to decrease. Maximum temperature at the outlet of the injector was 500 degrees C. This temperature is less than the temperature specification of 650 degrees C. Testing on consecutive days showed only very small amounts of carbon formed within the injector. The reduced temperature is used to curtail the formation of carbon as the diesel fuel undergoes heating and vaporization. This approach of using a reduced injector temperature requires that the diesel-steam mixture be heated to specification temperature once the diesel fuel is fully vaporized and dispersed into the steam.

4. *Laser system:* The laser system for diagnosing the completeness of vaporization and mixing at the outlet of the injector was set up and tested. The laser used is an argon ion laser, operated continuously with about 1 watt of power for the green line (514 nm). The laser Rayleigh scattering (LRS) method is used since it permits the degree of mixedness of the diesel vapor with the steam to be discerned. This is possible because the scattering cross-sections of steam and diesel vapor are very different. Steam weakly scatters the laser light, diesel vapor strongly scatters the light, and diesel-steam well mixed at the desired mass ratio scatters the laser light with an intermediate intensity. Thus, by measuring the rms fluctuation of the scattered light, and comparing it to the mean signal, it is possible to ascertain how well the injector has mixed the diesel fuel into the steam.

5. *Laser Rayleigh scattering measurements:* The outlet stream of the injector for the 1000 watts fuel cell was tested by the laser Rayleigh scattering method, following calibration of the method. This testing was performed with the injector operating at atmospheric pressure. Outlet temperature was varied up to approximately 500 degrees C. The steam mass flow was held at the nominal value, while the diesel mass flow was varied over a considerable range. Typically, the ratio of the rms to the mean of the scattering signal was approximately 0.1, indicating an acceptable mixedness of the diesel vapor with the steam. No evidence of carbon formation was found during these tests.

6. *Carbon formation:* Literature on carbon formation was reviewed and results from the literature were applied to assess the potential for carbon formation in the injector. Chemical process literature on the steam reforming of refinery hydrocarbons and gas turbine literature on diesel vaporizers were examined. These literature sources discuss the mechanisms of carbon formation, and indicate that carbon formation can be suppressed by maintaining the temperature of the steam-hydrocarbon mixture below about 650 degrees C and by eliminating the leakage of air into the mixture.

Advanced Fuel Injector for a Catalytic Micro-Channel Fuel Cell Processor

INTRODUCTION

Fuel cells have been proposed for cleanly and efficiently converting the chemical energy in hydrogen fuel into electrical energy. Unfortunately, hydrogen gas does not exist in nature and, therefore, it must be produced if fuel cells are to be used for electricity production. Hydrocarbon fuels, such as diesel fuel, are rich in hydrogen atoms that can be separated from the carbon atoms by reacting the fuel with steam in the presence of a catalyst. This process requires that the fuel be fully vaporized and mixed with the steam. The technology to atomize and vaporize liquid hydrocarbon fuels with air and steam is well developed for large, industrial systems, but little data are available on devices that vaporize and mix very small amounts of fuel with steam.

InnovaTek, Inc., under contract to the USDOE and the USDOD, is undertaking the development of an operational diesel-based fuel processor (reformer) to supply hydrogen for electrical generation by fuel cells. Such a reformer, combined with an appropriately sized fuel cell, is envisioned for the replacement of portable diesel field generators used in both civilian and military applications. As a stand-alone fuel processor, it will have significant potential for distributed hydrogen generation at stations for refueling fuel cell-powered vehicles.

The University of Washington, under research support from the Washington Technology Center and InnovaTek, Inc., has addressed the problem of preparing the diesel vapor-steam mixture for reaction in the catalyst of the fuel processor. It is desired for the mixture to exhibit a time-steady and spatially-uniform composition of diesel vapor and steam and to be free of carbon particulate and unvaporized, unmixed diesel fuel. The overall task is to develop an advanced diesel-steam injector, appropriately sized for the fuel cell applications of interest. The injector must accomplish atomization and vaporization of the diesel fuel and mixing of the diesel vapor with the steam.

Development of the advanced diesel-steam injector and evaluation of its performance were conducted at the University of Washington through a series of connected tasks. These tasks are:

1. Injector concepts and design, during which candidate concepts were studied and the injector was designed.
2. Experimental rig, during which the experimental rig for testing the injector was designed and built and the injector was built.
3. Injector testing, during which performance testing of the injector was conducted. This testing involved the measurement of temperatures, pressures, and steam and diesel flow rates within the injector system. Additionally, the carbon-forming tendency was examined.
4. Laser system, during which the argon ion laser system and the laser Rayleigh scattering (LRS) method were set up and debugged.

5. Laser Rayleigh scattering measurements, during which the outlet stream of the injector, operated at atmospheric pressure, was examined with the LRS method to study the vaporization and mixing goodness of the injector.
6. Carbon formation, during which literature on carbon formation in steam-hydrocarbon mixtures was examined and applied to ascertain the mitigation of carbon formation in the injector.

These tasks and their results are described in the subsequent sections of this report.

SPECIFICATIONS

InnovaTek, Inc. provided the design-point specifications for the steam and diesel flow rates and for the temperature and pressure of the diesel-steam mixture. For application to the catalytic micro-channel fuel processor originally envisioned for the 100 watts fuel cell, the specifications were:

- Steam mass flow rate: 0.013 to 0.039 grams/sec
- Diesel mass flow rate: 0.005 grams/sec
- Mixture temperature: 650 degrees C
- Mixture pressure: 70 psig.

As originally envisioned the injector was to have a rectangular cross-section of low profile, that is, the injector was envisioned to have a small height to width ratio. Such a design would likely have required multiple tiny jets of liquid fuel entering the injector. Early on, it was decided to change to a circular cross-section for the injector, with a single liquid jet. This injector and the appropriately sized experimental rig were designed and built.

Prior to testing this design, the flow rate specifications were changed to values appropriate to a 1000 watts fuel cell. The new specifications provided by InnovaTek, Inc. were:

- Steam mass flow rate: 0.2 to 0.4 grams/sec
- Diesel mass flow rate: 0.035 to 0.070 grams/sec
- Mixture temperature: 650 degrees C
- Mixture pressure: 70 psig.

Modifications were made to the injector and experimental rig to accommodate the factor 10 greater flow rates. This change made the design and fabrication of the injector somewhat easier, since it was no longer necessary to deal with the very low flow rates and dimensions. Testing of this injector was performed.

Because of the concern about carbon formation at high temperature, it was decided to limit the maximum temperature in the injector to 550 degrees C. This led to mixture temperatures of 300 to 500 degrees C at the outlet of the injector. By this approach, it will be necessary to insert a heater between the injector outlet and the catalyst inlet to bring the mixture to the desired high temperature for catalytic reforming. It is conjectured that rapidly heating the mixture to high temperature after the diesel fuel has been fully dispersed into the steam should curtail the tendency to form carbon.

INJECTOR CONCEPTS AND DESIGN

Candidate injector concepts were examined using computational fluid dynamics (CFD). This was done using the specifications for the 100 watts fuel cell. Hexadecane fuel, added as 10 microns droplets, was assumed as a surrogate for the diesel fuel. Prior to running the CFD calculations, it was necessary to examine the vaporization times of the fuel droplets and adjust the vaporization parameters of the CFD code so that textbook vaporization calculations could be matched. Example vaporization results are shown below, followed by the CFD results for the candidate designs. Then the design of the injector selected is shown and discussed.

Vaporization time calculations

Example results computed for the vaporization time are shown below in the two-part figure (Figure 1). These results pertain to the vaporization of a single droplet of the model fuel compound hexadecane ($C_{16}H_{34}$) exposed to the static environment of steam at 650 degrees C and 70 psig. The initial droplet diameter is 10 microns, which is a relatively small diameter for liquid fuel atomized by a nozzle. Two situations are treated, one in which the Lewis number remains fixed at unity, which is commonly assumed in calculations of this type, and the other in which the Lewis is variable and is evaluated from the transport properties. The Lewis number is defined as the ratio of the thermal diffusivity to the mass diffusivity. It indicates the relative ease with which heat from the surrounding medium diffuses to the droplet, and thus, is available to drive the vaporization process, over the ease with which fuel vapor diffuses from the droplet into the surrounding medium.

The right-side part of the figure shows the change in the temperature of the droplet as it heats up from room temperature to its steady state temperature. The left-side part of the figure shows the change in the mass of the droplet as it vaporizes. The key findings are as follows:

- The droplet reaches a steady state temperature of about 560 K (or 290 degrees C).
- The overall droplet evaporation time is about 1 millisecond (ms).
- Much of the evaporation occurs as the droplet heats up. A relatively small amount of evaporation occurs after the droplet reaches its steady-state temperature. This is a different situation than that occurring when droplets are exposed to a gas of temperature in the 300-500 degree C range, in which case the portion of the evaporation at steady-state temperature is more pronounced and tends to dominate the overall vaporization process.
- The Lewis number decreases from about 3 at the start of vaporization to about 0.7 at the conclusion of vaporization.

Calculations have also been performed for a 30 microns droplet. This exhibits a steady-state temperature essentially identical to that of the 10 microns droplet. The Lewis number behavior is also nearly identical to that of the 10 microns diameter droplet. Of most importance, the evaporation time scales as D^2. Thus, the evaporation time for the 30 microns droplet is about 10 ms. Although a 100 microns droplet has not been modeled, application of the D^2 rule indicates it would exhibit an overall evaporation time of about 100 ms.

The maximum droplet size produced by the atomization process of the injector is unlikely to exceed 100 microns. Thus, the evaporation time should not exceed 100 milliseconds. Of course, the use of steam cooler than 650 degrees C will increase the vaporization.

Significant information is available in the literature regarding the vaporization of hydrocarbon fuels (both pure and blended) in air. However, less information is available on vaporization of hydrocarbons in steam. Thus, we have based our analysis on the procedures established for air, and substituted the steam properties for the air properties. The procedure carries with it simplification of the real-gas effects that occur in high-pressure hydrocarbon vapor-steam mixtures.

The largest steam flow and largest droplet size put the greatest demand on the selection of the injector length. A tube of 1 cm diameter and 4 cm length will provide a gas residence time of 100 to 120 milliseconds for the high flow case (of 0.005 plus 0.039 grams/sec). Additional length will be required for mixing of the fuel vapor and steam. An injector tube of 1 cm diameter and 10 cm length should provide adequate residence time for vaporization and mixing the fuel and steam. The exact length will depend on the results of the CFD modeling, in particular, the modeling of the mixing of the fuel vapor with steam.

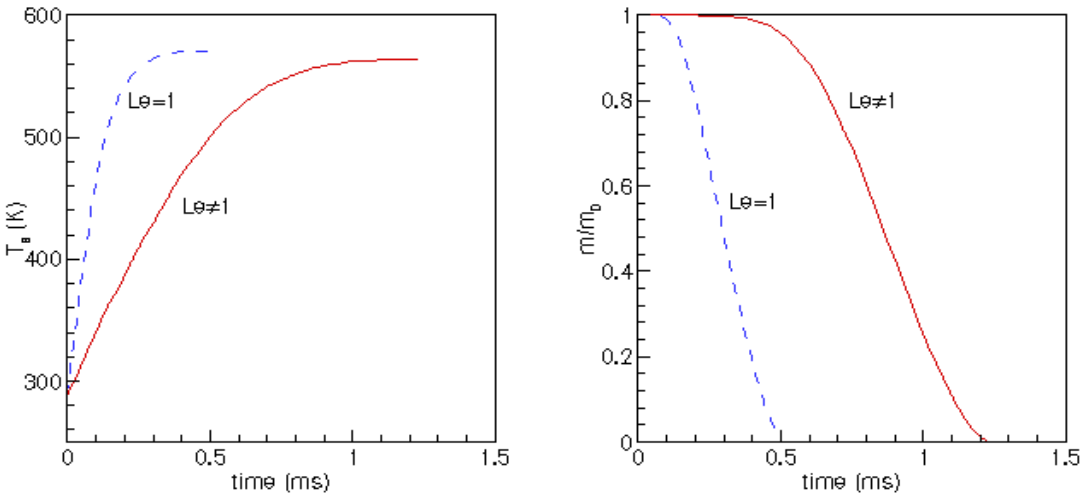

Figure 1. Temperature and mass fraction remaining for a 10 microns droplet vaporized in steam at 650 degrees C and 70 psig

CFD calculations of candidate injectors

The CFD calculations of the candidate injector concepts used the following parameters – essentially the InnovaTek specifications for the 100 watts fuel cell:

- 5 mg/s and 7 mg/s fuel flow rates
- 13 mg/s and 40 mg/s steam flow rate
- 650 C mixture temperature when mixing is complete
- 585 kPa nominal absolute mixture pressure
- $C_{16}H_{34}$ fuel composition

Considerations include:

- Minimal heat loss
- Minimal pressure drop
- Rapid vaporization
- Good mixing between steam and fuel

The production of a uniform mixture of vaporized fuel and steam can be divided into three stages: atomization of the fuel, vaporization of the fuel, and mixing of the fuel vapor and steam. Lefebvre (1989) discusses the first stage in detail. In summary, an atomized fuel spray is commonly produced by forcing the liquid fuel through a small orifice and then subjecting it to a high speed flow of gas so as to establish a shear flow that tears the fluid droplets apart. An alternative approach involves wetting with fuel a surface that is parallel to the direction of the gas flow. Using dimensional analysis and results from experiments involving liquid fuels and air, Kihm et al. (1995) suggest that the droplet diameter produced by cross-injecting sprays into a convective stream should be a function of the orifice diameter, the fuel and gas Reynolds numbers, and the Weber number, which relates the viscous force to the surface tension force.

The second stage of the process, vaporization, is dominated by the rate at which heat can be transferred into the fuel droplet through its boundary layer. Since the droplet has little mass, the differential velocity between the droplet and the gas will be almost zero and the heat transfer process is dominated by diffusion rather than by convection. If the surrounding gas flow is quiescent and the fuel-gas mass ratio is not extremely small, the vaporization of the fuel will cause the gas temperature around the droplets to be reduced, thereby slowing the rate of vaporization of the fuel. Therefore, vaporization will occur faster if the gas is well mixed. Mixing of fluids occurs through diffusion and advection and the ratio of the time scales for these two mechanisms is the Peclet number. The Peclet number is analogous to the Reynolds number and the two differ by a multiplicative constant of order one for fluids with constant properties.

From the preceding comments, it is concluded that the time required for each of the three stages of the atomization-vaporiztion-mixing process should decrease with increasing fuel and gas Reynolds numbers. In particular, we expect the second two stages to occur fast if the flow is turbulent. There are no criteria for predicting whether an arbitrary flow will be turbulent, but we can consider the case of flow in a pipe, which approximates the flow that would occur if a jet of fuel were injected into co-flowing steam in a circular duct. Flow in a pipe transitions from laminar to turbulent at a

Reynolds number of about Re_D=2300, where Re_D=UD/ν, U is the mean velocity, D is the diameter of the duct, and ν is the kinematic viscosity of the fluid. For the current flow rates, D≅0.2 mm would be required for the flow to have a high enough Reynolds number for it to transition from laminar to turbulent. Such a small duct is not practical: it would be difficult and costly to manufacture, it is only three to five times the diameter of fuel particles produced by typical fuel atomizers which makes the fluid dynamics in the duct very difficult to predict, and the duct would be readily susceptible to fouling by contaminants in the fuel or steam. Therefore, it is concluded that establishing a turbulent flow for vaporizing the fuel droplets and mixing the fuel vapor with steam is not a practical approach in the current application. This conclusion is validated by the first of the three injector configurations examined below.

It is worthwhile to comment on the characteristics of jets since jets are commonly used for mixing two fluids. Like other flows, jets can be turbulent or laminar. In a turbulent jet, instabilities around the perimeter of the jet cause vortices that entrain fluid from the surrounding flow. The jet grows in diameter as it moves downstream from its source because mass is entrained into the core flow. A turbulent jet will readily grow provided that a source of fluid is provided for it to entrain. Therefore, a turbulent jet of fuel will readily entrain surrounding steam and produce a uniformly mixed flow fairly quickly. A laminar jet, on the other hand, grows only by molecular diffusion of surrounding fluid into the core flow. Since diffusion is a much slower process than turbulent advection, laminar jets grow more slowly and are much less effective at mixing two fluids than are turbulent jets.

The present problem of producing a well-mixed, low Reynolds number flow of vaporized fuel and hot gas is similar to that studied by Lee (2000). In his case, the objective was to test a design for a gas turbine injector by evaluating a laboratory-scale version of the device. The fuel and air flow rates were 56 mg/s and 1333 mg/s, respectively, which are significantly higher than the flow rates in the current research but are much lower than those in the industrial applications discussed in Lefebvre (1989) and other literature. It is, therefore, informative to examine the design of Lee's device called the Staged Prevaporizer-Premixer (SPP) and shown below in Figure 2. In the SPP, the fuel enters through a small tube shown near the bottom of the diagram. Surrounding this tube is another small tube that carries atomizing air. Most of the air, however, enters the SPP through the first and second stage air inlets. The first stage air inlet directs the flow around the outside of the tube carrying the atomized fuel and serves to keep the fuel droplets away from the walls of the SPP and to provide air for the fuel jet to entrain. The second stage air enters as an array of turbulent jets that rapidly mix with the fuel-air mixture from the first stage. Examination of the gas at the exit of the SPP shows that the device is very effective at producing a uniform mixture of vaporized fuel and air.

In the SPP, the air is introduced at two locations in order to prevent the premature oxidation of some of the fuel components before the gas is injected into the burner. With a fuel-steam mixture, this is not a consideration and a two-stage approach is not required. However, a single-stage injector based on the first stage of the SPP provides

a convenient starting point in the design of a device for the current problem. configuration 1 below considers an SPP-like design for use as a fuel-steam injector.

Configuration 1: The first injector design consists of a steam inlet tube and a mixing chamber connected by a 0.2 mm diameter orifice. A fuel inlet tube, not considered in the simulation, delivers the fuel just upstream of the orifice. The steam and fuel then flow through the orifice at about 0.6 times the speed of sound. Based on large-scale pressure atomizers, the transit through the orifice will atomize the fuel into droplets no larger than 50 μm. Additional steam flow (half of the total steam flow) is admitted through an annulus in the upstream wall of the mixing chamber (the annulus is concentric with the orifice). The jet issuing from the orifice and the additional steam entering through the annulus undergo mixing in a weak turbulent jet in the mixing chamber. The model geometry is shown in Figures 3 and 4.

In order to evaluate the performance of the injector, we first consider how well the fuel and steam mix by observing fuel mass fraction versus downstream distance. In Figure 5, contour plots of the fuel vapor mass fraction on a plane along the centerline of the device are shown. The case shown is for steam and fuel mass flow rates of 13 and 5 mg/s, respectively, so that the average fuel mass fraction is 0.266. The injector is very effective at producing a uniform mixture at a downstream distance of about 30 mm. Note that there is an intense recirculation zone that carries mixed steam and fuel from the exit all the way back to the upstream wall of the mixing chamber.

While this injector design yields a well-mixed gas at the exit, the pressure drop across the orifice is high. Contour plots of total gage pressure, referenced to zero pressure at the exit, are shown in Figure 6. About 150 kPa are lost between the steam inlet and the outlet. The large pressure drop occurs primarily at the inlet of the orifice. The upstream edge of the orifice could be modified to reduce the pressure drop, but the basic design of this injector is controlled by the high velocities used to atomize the fuel and produce a turbulent jet downstream of the orifice. A modification would be to increase the diameter of the atomizing, seeking a compromise between atomization and pressure drop.

Configuration 2: The second injector design consists of a steam inlet tube and a mixing chamber connected by a tapered nozzle. See Figure 7. The fuel is injected through the side of the nozzle at a right angle to the steam flow. Construction of the nozzle would require significant machining but the routing of the fuel tube might be simpler than in configuration 1. Also, it would be easier to keep the fuel tube cool in this design and thereby prevent vaporization of the fuel in the line and subsequent vapor lock. The pressure drop across the device is small with about a 0.55 kPa total pressure drop between the inlet and the outlet. Contour plots of the total gage pressure referenced to the outlet plane are shown in Figure 8.

Contour plots of the fuel vapor mass fraction in the injector and at the exit plane are shown in Figure 9. In the top and middle panels of the figure, the poor mixing typical of a laminar flow is evident. The steam jet coming through the nozzle from the left is

deflected downward by the momentum of the droplets entering through the narrowest point of the nozzle from the top, but little mixing occurs between the fuel and steam streams. The little mixing that does occur appears to be due to the fluid transport caused by the large volumetric expansion of the fuel as it evaporates. The bottom panel of the figure shows the mass fraction of the fuel vapor at the exit plane (note the orientation of the axes). The variation in the fuel vapor mass fraction across the exit is more than 2%. The conclusion that can be drawn from this design is that, while utilizing a laminar jet results in low pressure drop, the mixing of the fuel and steam is poorer than with configuration 1. Figure 10 shows the temperature contours.

Configuration 3: In configuration 3, we focus on developing a fluid flow that results in good mixing without turbulence. One characteristic of a poorly mixed fuel and steam stream is that there will be variations of temperature, and, therefore, variations of density, across the flow. The temperature field for configuration 2, shown in Figure 10, confirms this argument. Mixing a density stratified flow can be accomplished by accelerating the flow in a direction normal to the stratification which, in the case of a flow through a tube, involves inserting a bend in the tube in the appropriate plane. The bend will impart some vorticity into the flow, which will further enhance mixing.

Accelerating a stratified flow to cause mixing is used in configuration 3, shown in Figure 11. This design consists of steam and fuel inlet tubes that intersect at a right angle. A 0.2 mm orifice (the smallest that can be reasonably manufactured), is inserted in the fuel tube to produce a fine stream, or a droplet array, of fuel. Downstream of the junction of the two inlet tubes is the mixing tube, which is S-shaped to promote mixing. Contour plots of the fuel vapor mass fraction for the case of steam and fuel flow rates of 40 mg/s and 7 mg/s, respectively, are shown in 12. The fuel and steam are mixed at the exit plane to within 0.2%. The drop in total pressure across the device is 0.11 kPa.

The temperature on the centerline plane is shown in 13. The steam and fuel enter the injector at 923 K and 300 K, respectively, and the tube walls are considered to be perfectly insulated. Heat conducts along the walls, which are modeled as 3 mm thick 316 stainless steel, so that the fuel heats up before it mixes with the steam. The average temperature of the mixture at the exit of the injector is 825 K.

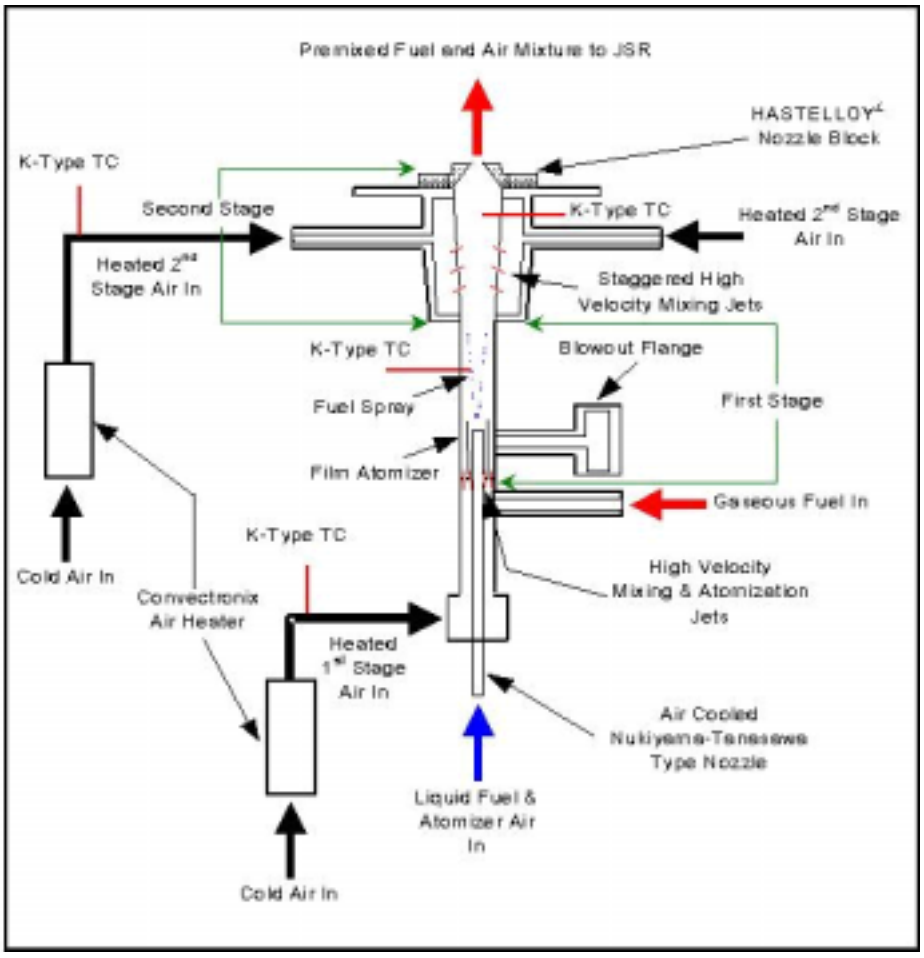

Figure 2: Schematic of the Staged Premixer-Prevaporizer (Lee, 2000)

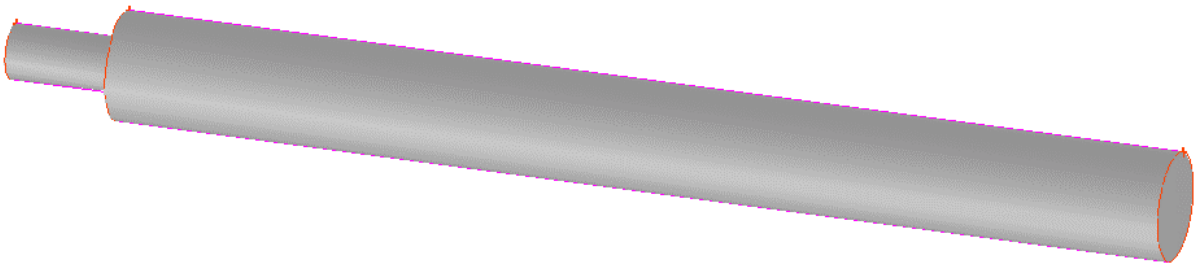

Figure 3: View of configuration 1

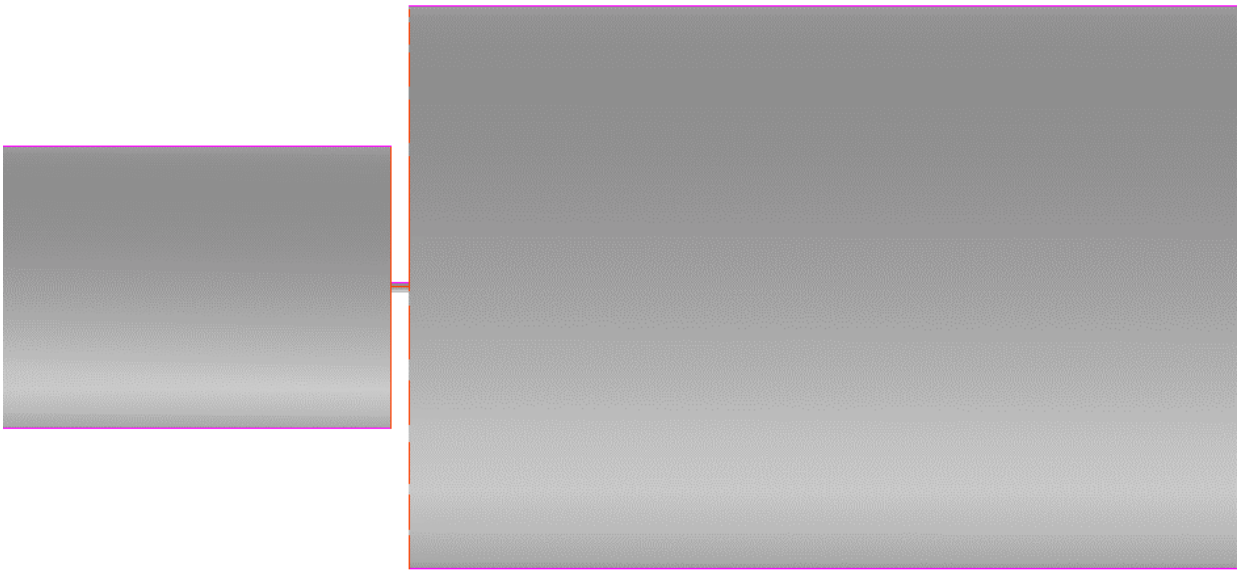

Figure 4: Close-up view of configuration 1 showing orifice through which fuel and steam are injected into the mixing chamber.

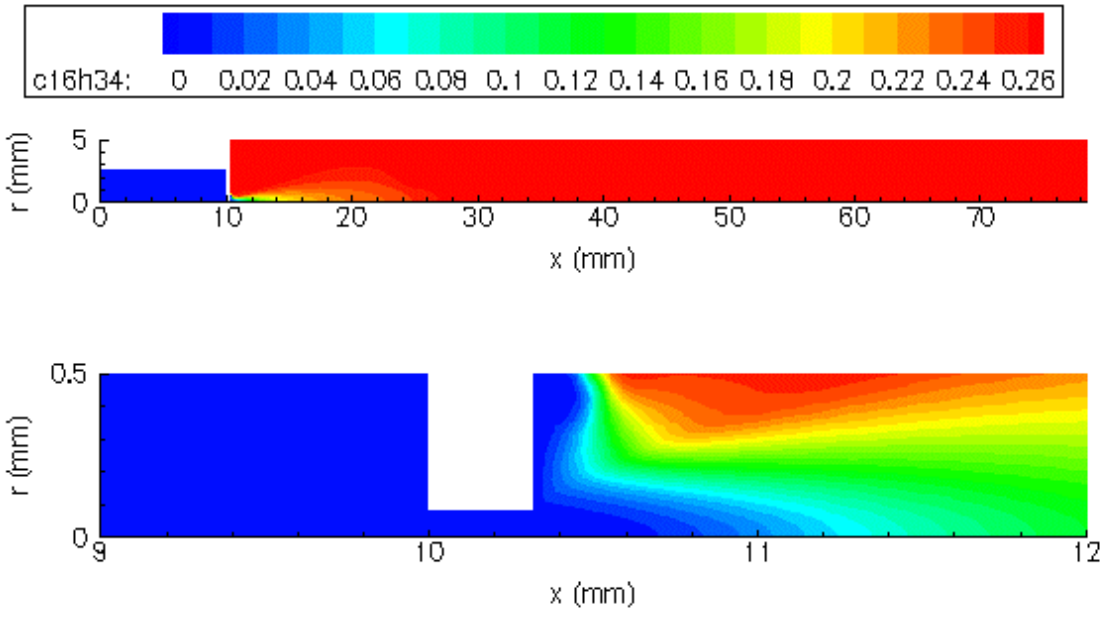

Figure 5: Fuel vapor mass fraction along centerline plane of configuration 1. Fuel and steam flow rates are 5 mg/s and 13 mg/s, respectively.

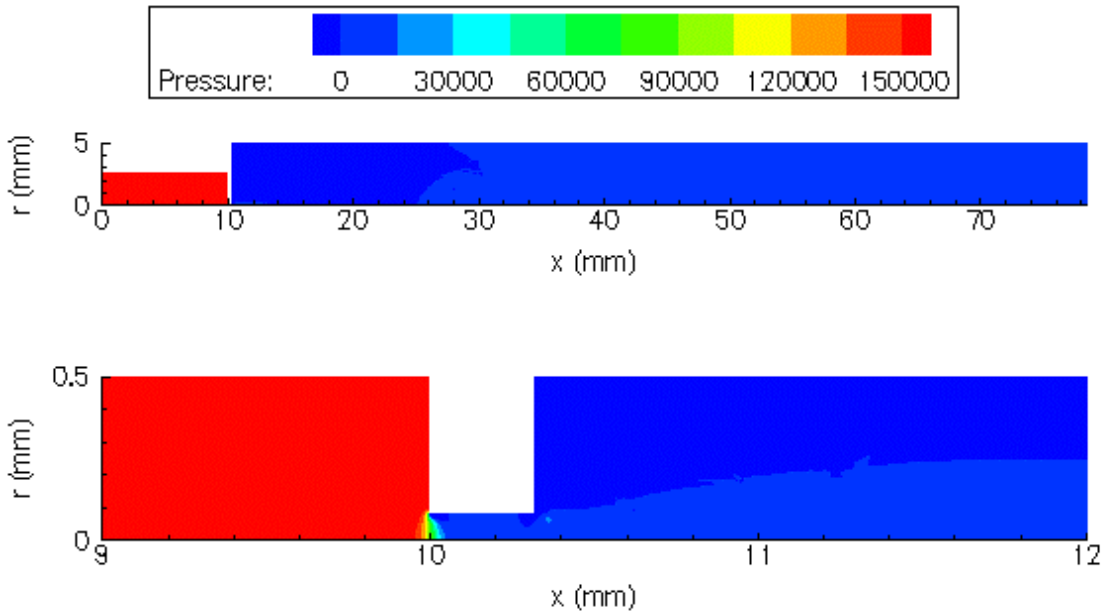

Figure 6: Total gage pressure (Pa) along centerline slice of configuration 1. Fuel and steam flow rates are 5 mg/s and 13 mg/s, respectively.

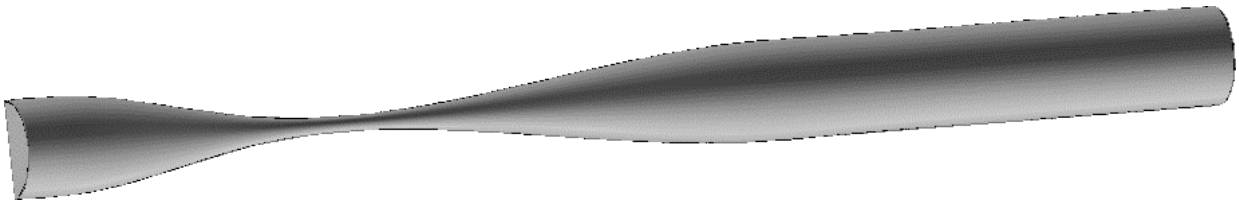

Figure 7: View of configuration 2

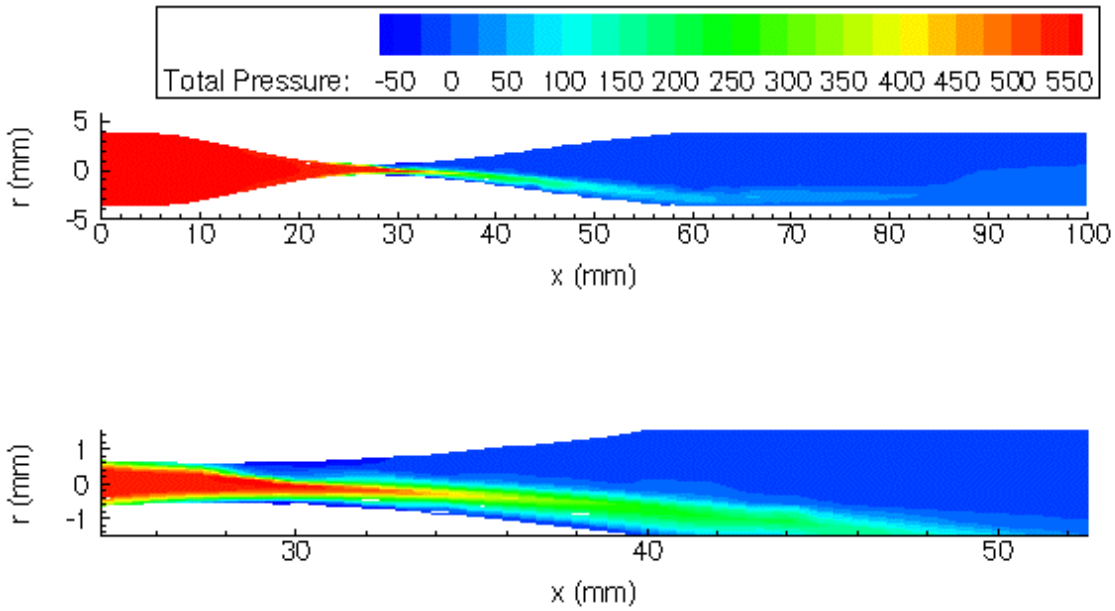

Figure 8: Total gage pressure (Pa) along centerline plane of configuration 2. Fuel and steam flow rates are 5 mg/s and 13 mg/s, respectively.

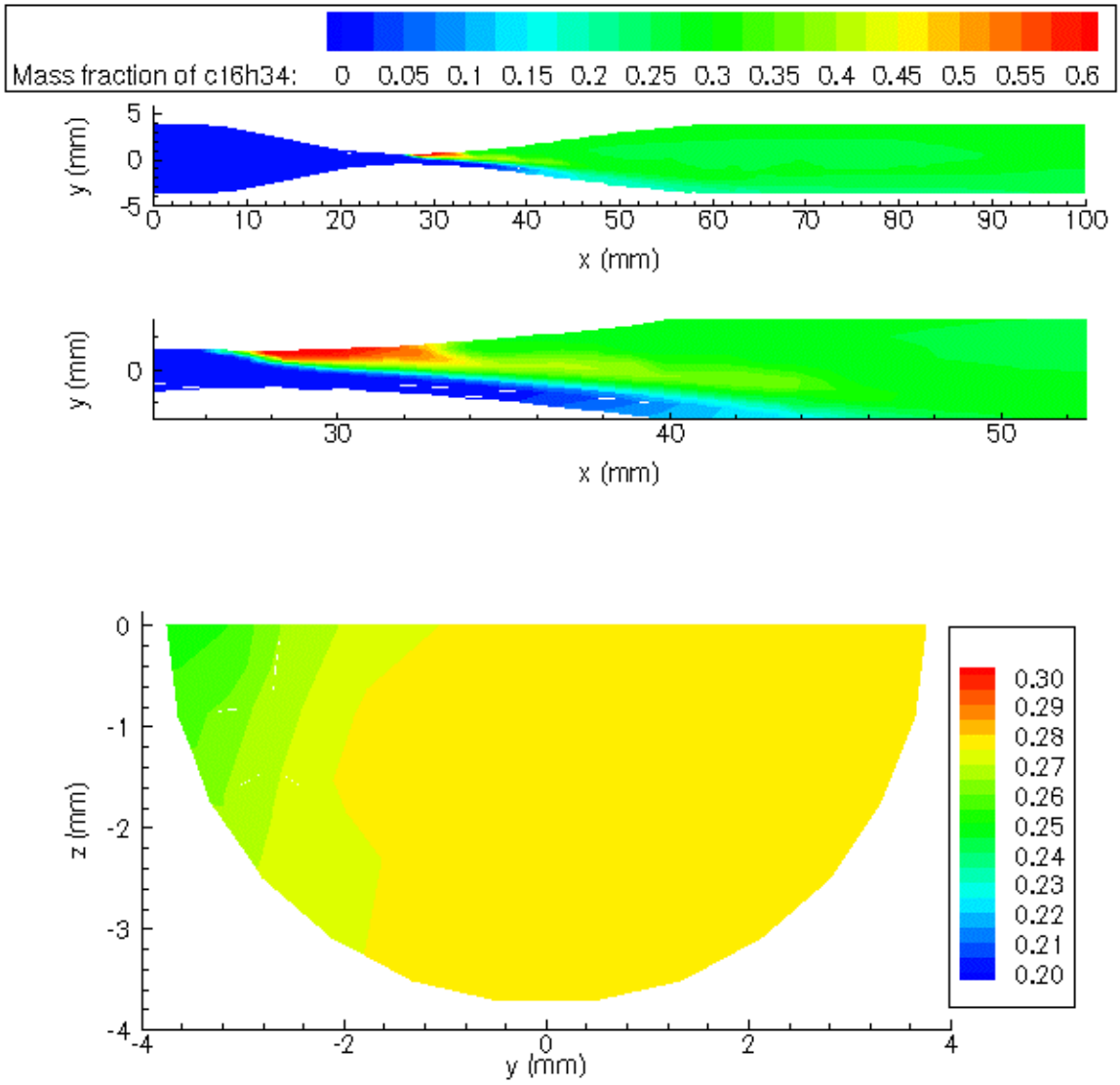

Figure 9: Fuel vapor mass fraction along centerline plane and on exit plane of configuration 2. Fuel and steam flow rates are 5 mg/s and 13 mg/s, respectively.

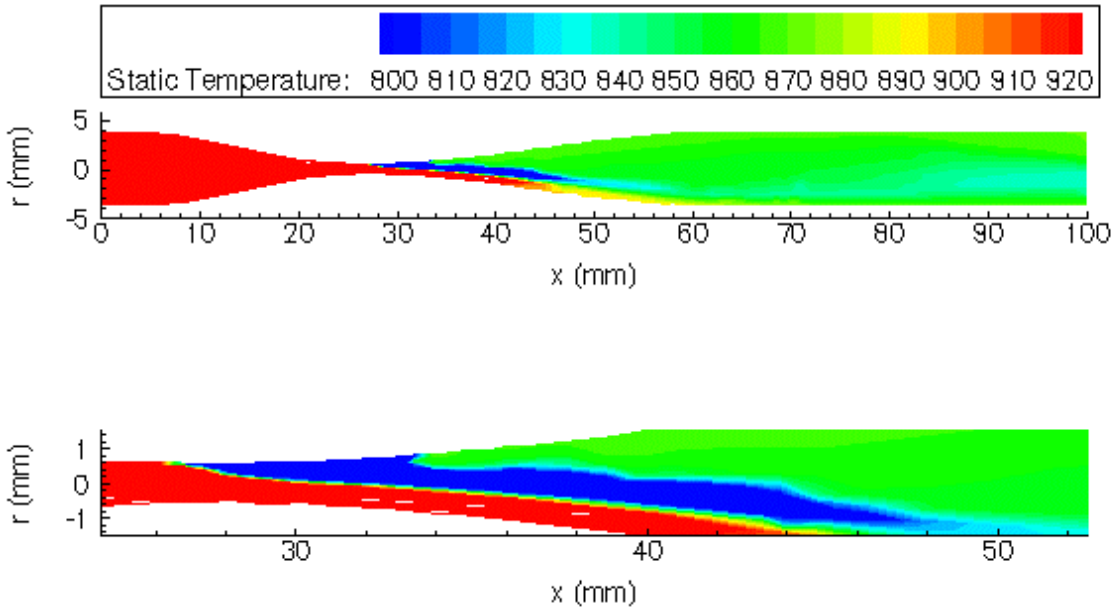

Figure 10: Temperature along centerline plane of configuration 2. Fuel and steam flow rates are 5 mg/s and 13 mg/s, respectively.

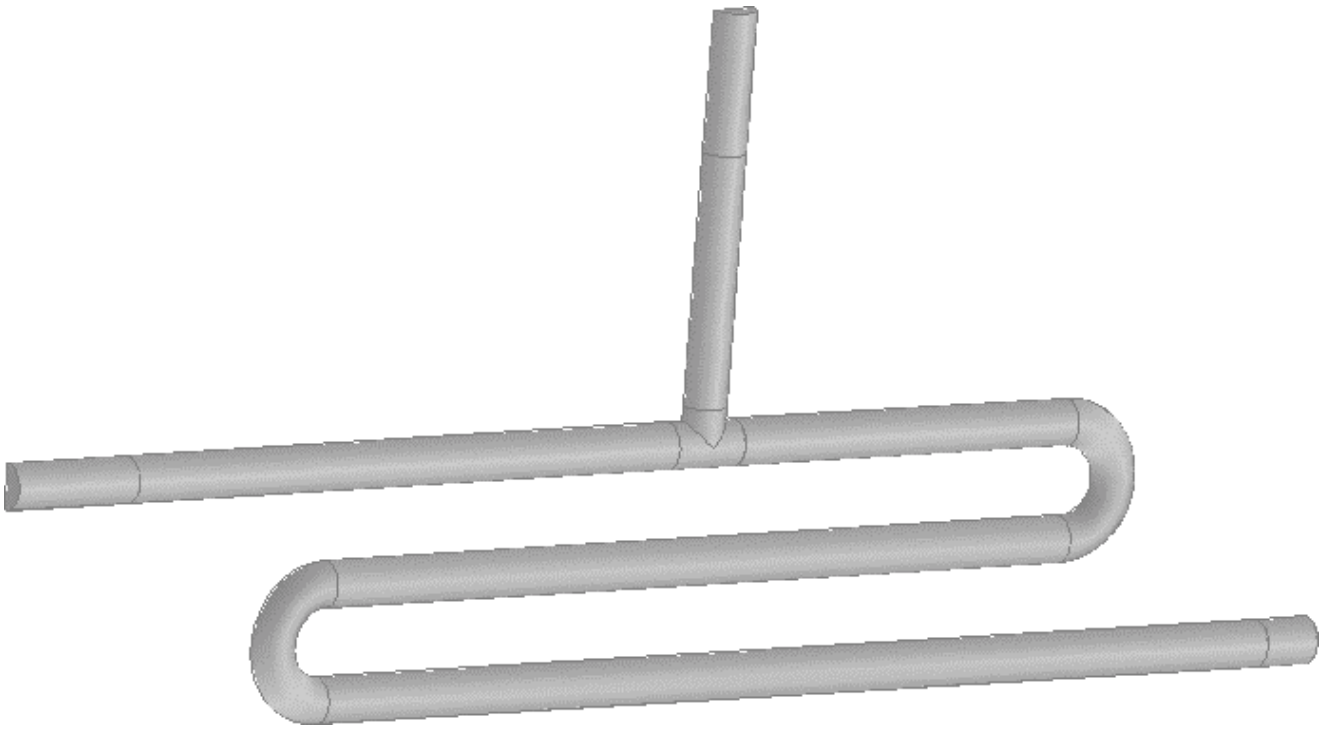

Figure 11: View of configuration 3

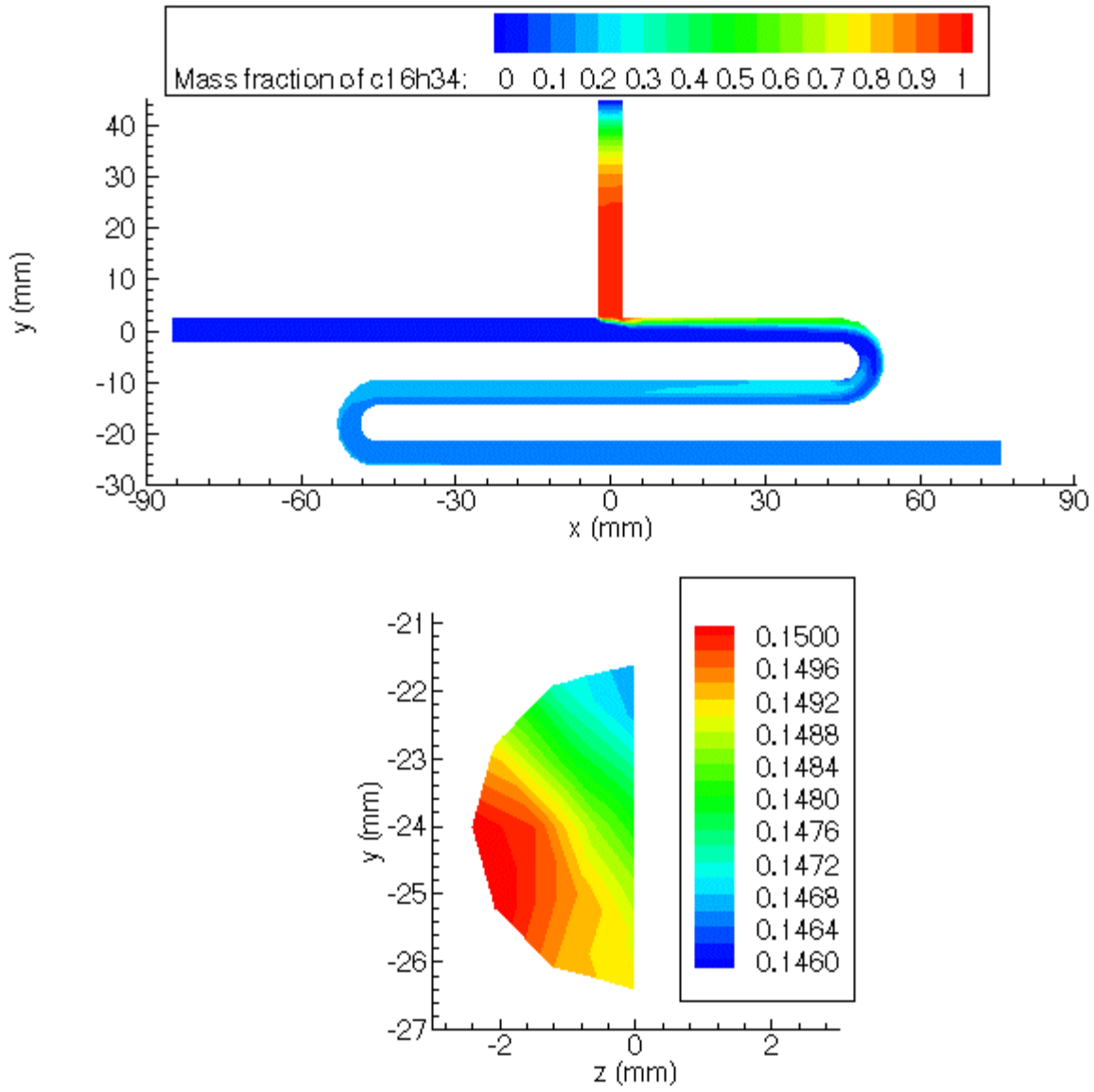

Figure 12: Fuel vapor mass fraction on centerline plane and at the exit plane of configuration 3. Fuel and steam flow rates are 7 mg/s and 40 mg/s, respectively.

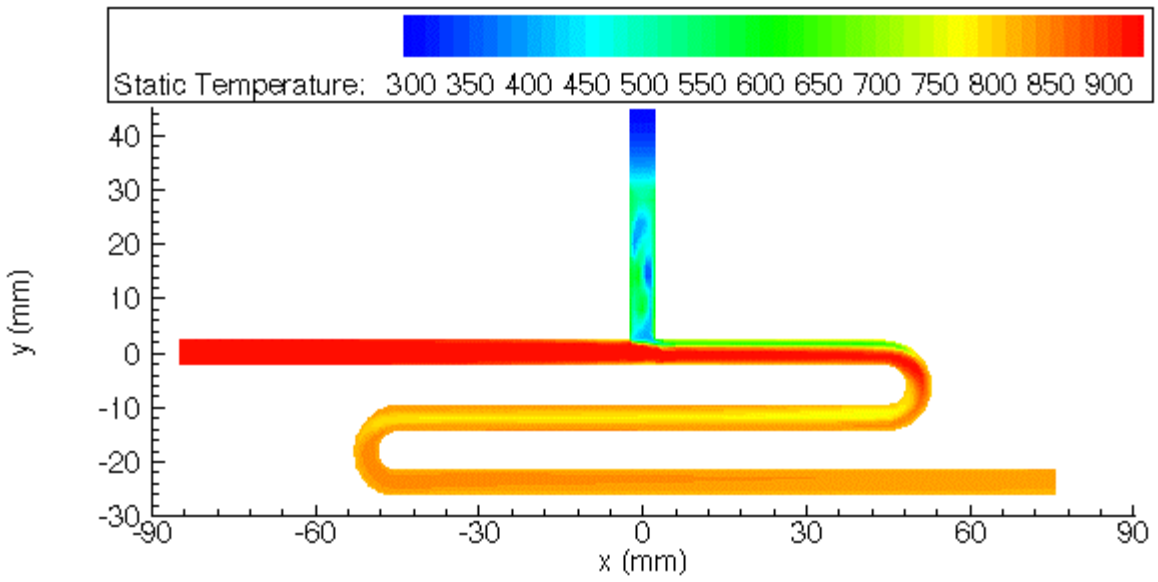

Figure 13: Temperature along centerline plane of configuration 3. Fuel and steam flow rates are 7 mg/s and 40 mg/s, respectively.

Injector design

Configuration 1 was chosen as concept for the design of the injector. This configuration should minimize carbon deposit formation and is relatively inexpensive to fabricate. Configuration 2 would be expensive because of the contoured nozzle, and configuration 3 could suffer from carbon formation in the fuel feed tube.

Configuration 1, as shown in Figures 3, 4, 5, and 6 above, has two chambers connected by a narrow nozzle. The upstream chamber is the steam plenum, and the downstream chamber is the vaporization and mixing tube. The design is based on the plain-jet atomizer discussed in Lefebvre (1989) and used by Lee (2000). In the design of configuration 1 shown in Figure 14 below, the diameter of the atomizing nozzle has been increased two-fold from that assumed in the CFD modeling, and the fuel tube carrying the pressurized liquid diesel fuel is inserted into the plenum. Liquid diesel fuel is jetted through a tiny orifice at the exit of the fuel tube, about 2 mm upstream of the atomizing nozzle that connects the two chambers. The liquid jet is accelerated through the nozzle by steam rushing through the nozzle. The high velocity steam shears the liquid fuel jet. Atomization of the liquid fuel jet is accomplished in two ways: 1) by the tiny orifice at the fuel tube exit, and 2) by the shearing action of the steam in the nozzle.

The injector shown in Figure 14 was designed for a diesel flow of 7 mg/s and a steam flow of 40 mg/s. The plenum design conditions are 90 psig and 500 degrees C of steam. Pressure drop occurs across the nozzle, resulting in a final pressure in the injector tube of 70 psig. In order to reach the design point temperature of 650 degrees C, the steam-diesel vapor mixture must be heated downstream of the injector prior to the catalyst.

Because of the very small flow of diesel fuel, a potential problem with this design is vapor lock in the fuel tube carrying the liquid diesel. In order to overcome this, the fuel tube must be cooled. Furthermore, the fuel tube must be inserted into the steam plenum only a relatively short distance. This necessitates a steam plenum of short length (of about 2 cm).

Another potential difficulty is the tiny diameter of the fuel tube orifice, of about 0.2 mm. This requires filtering of the diesel fuel.

Drawing of injector built for testing

The drawing of the injector built for testing with 7 and 40 mg/sec of diesel and steam, respectively, is shown in Figure 14. This injector was fabricated in the UW Mechanical Engineering Shops. The material is 316 SS. From left to right in the Figure 14, the parts are as follows:

- Water-cooled fuel tube. At the left end of the tube, the liquid fuel enters the steam environment though the small outlet. Ruby nozzles of 75 microns diameter or less, available as the tips for micro torches, are used

at the outlet of the fuel tube. These provide a fine liquid jet for entry into the atomizing nozzle.

- Steam plenum and nozzle. This part is shown in the center of the drawing. The jet of fuel exiting the fuel tube encounters steam and the fuel-steam mixture accelerates though the atomizing nozzle. An enlarged view of this is shown in the drawing. This is the "heart" of the injector. The nozzle hole is drilled in the nozzle block made of porous stainless steel. (Although not stated on the drawing, solid stainless steel is also used.) Six nozzle blocks were made for testing. The materials were 2 micron porosity stainless steel (SS), 40 micron porosity SS, and solid SS. Each of these nozzle blocks is drilled with either a 0.2 or 0.4 mm hole. The design diameter is 0.4 mm, while the 0.2 mm diameter is using for comparison. The stream of diesel fuel co-flowing with steam is accelerated through the nozzle. With the use of the porous SS nozzle blocks, some of the steam flow through the porous material, thereby maintaining the downstream side of the nozzle block free of fuel and carbon deposits. Steam enters the plenum though the side port of the plenum. A ¼" tube – ¼" NPT Swaglok connector is used at this point to connect the injector to the steam generator (discussed in the next section of this report).
- Vaporization tube. This SS tube has an id of 4.7 mm and a length of 75 mm. The tube is sized to provide a nominal residence time of 100 milliseconds for the fuel-steam mixture. The tube length can be changed as found to be necessary.
- Measurement cell. At the far left of the drawing, one notes the measurement cell. This contains NPT threaded holes for inserting the thermocouple probe and the line to a pressure gauge. For testing, the backpressure plate with a tiny orifice is connected to the outlet of the measurement cell. The orifice diameter is selected to provide the 70 psig pressure in the vaporization tube of the injector.

The injector can be readily disassembled for inspection – looking for carbon deposits. It is also relatively easy to modify.

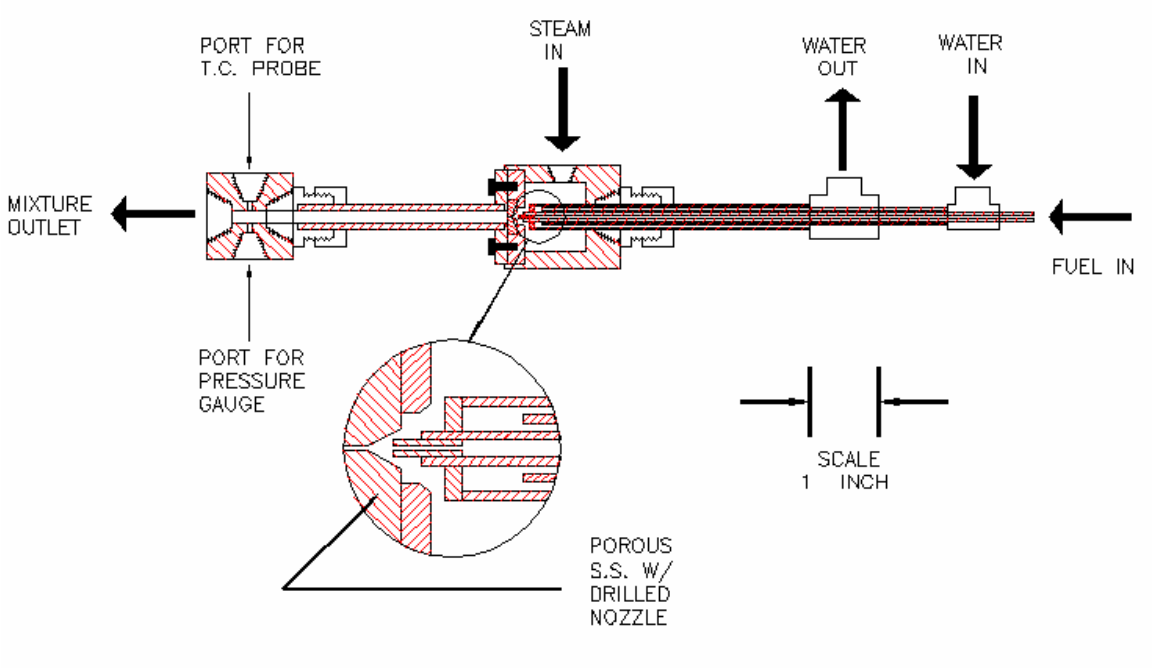

Figure 14: Design of the injector built for testing with diesel and steam flows of 7 and 40 mg/s, respectively.

Near the end of the 3rd quarter of the project, it was necessary to design and modify the injector because of the change to a 10-fold larger fuel cell size than originally assumed. The original application was for 100 watts fuel cell, while the new application was for 1000 watts. Although the basic design of the fuel cell remained as depicted in Figure 14, the following critical components were changed to the following dimensions:

- A mini torch tip with ruby orifice is used at the end of the fuel tube to provide a fine jet of the fuel. The orifice is 150 mm in diameter and it gives a ~50 mm long diesel jet at the flow-rate of 30mg/s at 1atm.
- Atomized nozzle of solid stainless steel: 0.80 mm diameter.
- Vaporization tube: 135 mm length, 9.5 mm outside diameter, and 7.1 mm inside diameter.

This modified injector was used in the testing phases of the project, as described later in this report.

EXPERIMENTAL RIG

The experimental consists of the following major components:

- Tank of distilled water, in which the water is kept under N_2 pressure.
- Rotometer and control valve for monitoring and metering the flow rate of water into the boiler of the steam generator.
- Steam generator, consisting of:
    - Boiler, fitted with electrical cartridge heater, thermocouple sensor, and burst disk.
    - Superheater, fitted with electrical cartridge heater, and thermocouple.
    - Power controllers.
    - Temperature/process controllers.
- Tank of diesel fuel, in which diesel fuel is kept under N_2 pressure.
- Rotometer and control valve for monitoring and metering the flow rate of diesel fuel into the injector.
- Injector, shown in Figure 14, supplied with high pressure, superheated steam and with high pressure diesel fuel.
- Backpressure orifice attached to the exit of the injector.

The injector, for the 100 watts fuel cell application, has been described in the previous section of the report. The steam generator, for the 100 watts fuel cell case, is described as follows.

Steam generator

The steam generator layout is provided in Figure 15. Water at room temperature enters the boiler and is vaporized by the 200 watts cartridge heater. Saturated steam at about 170 degrees C exits the boiler and enters the superheater. The boiler is insulated. By causing a small pressure drop between the boiler and superheater, the steam is dried. In the superheater, a 100 watts cartridge heater increases the steam temperature to over 500 degrees C without significantly losing pressure. The superheated steam moves to the injector.

The electrical heaters are controlled by the power controllers, which take signals from the temperature/process controllers and send adjusted power to the heaters. A T/P controller is capable of accepting universal process signals such as 4-20mA and 0-5Vdc and of transmitting universal signal as an output.

Testing of steam generator

The steam generator was tested for the conditions required for the 100 watts fuel cell application, and was found to perform satisfactorily. With a 0.2 mm diameter orifice placed at the outlet of the steam generator (see Figure 15), it was found possible to reach a pressure of 100 psig. The steam flow rate was 40-50 milligrams per second.

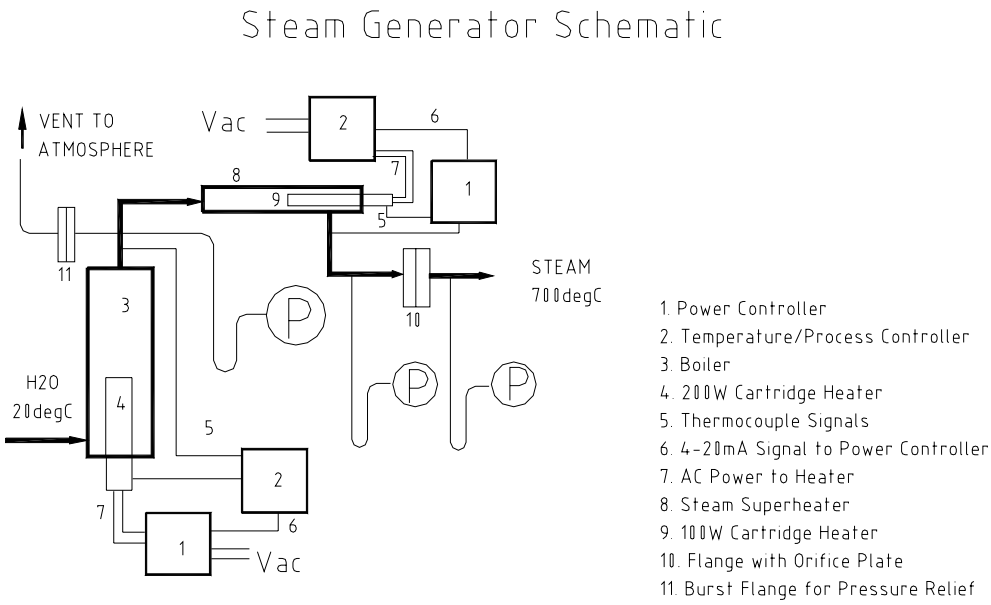

Figure 15. Schematic of electric steam generator

Two photographs of the steam generator are shown below. The first photo (Figure 16) is a front view of the rig, showing the temperature controllers. Also seen are the pressure gauges and fuel rotometer. Seen on the left side of the rig is the nitrogen tank for pressurizing the water and fuel vessels. Also noted at the left, behind the front panels, is the water vessel. At the right, and behind the front panels, the insulated steam generator is seen. The second photo (Figure 17), shoot from the right side of the rig, shows the insulated steam generator. Attached to outlet is the 0.2 mm backpressure orifice plate.

Figure 16: Front view of steam generator

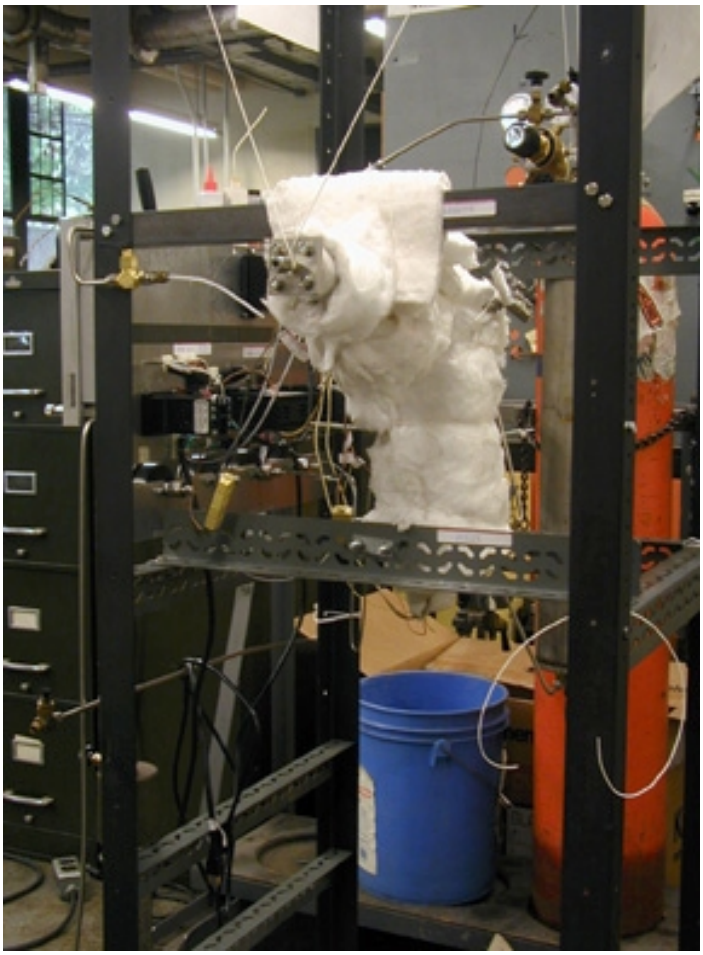

Figure 17: Right-side view of steam generator showing insulated steam generator

Design of new steam generator

Upon learning of the change from the 100 to 1000 watts fuel cell application near end of the 3rd quarter of the project, design of an enlarged steam generator with enlarged cartridge heaters was begun. New heaters were obtained, with ratings of about 2 kw for the boiler (requiring 208 volts) and about 0.5 kw for the superheater. The new steam flow rates are 10-fold higher than the nominal flow rate of the previously developed steam generator. The previously developed steam generator was undersized for the new flow rates.

TESTING OF INJECTOR

Initial testing

At the beginning of the 4th quarter of the project, initial testing of the re-designed and re-built steam generator was carried out for new steam/diesel flow-rates. The injector was modified with the new, enlarged ruby tip at the exit of the fuel tube and with an enlarged atomizing nozzle, though the vaporization tube was not changed from the original design. Once the new 208 volt heater arrived and was installed in the boiler, and the super-heater heater was upgraded to 500 watts, it was possible to reach the desired steam flow rate of 200 mg/s. The 200/35 case corresponds to a 500 watt fuel cell application. Following are summaries of the experimental setup and the results of the 200/35 (mg/s) testing.

Setup:

- The system consisted of three main components: boiler, super-heater, and injector.
- The new boiler holds 2.6 liters of water, though only 2 liters of water were pre-filled for each test. Make-up water was added as needed from the auxiliary reservoir – then the boiler was capable of generating 200mg/s of steam for approximately 5 hours.
- Store-quality distilled water was used to make steam and off-road #2 diesel was used as the fuel.
- The cartridge heater used in the boiler has a diameter of 19 mm and a heated length of 150 mm. The rated power is 2.4 kw at 240V and 1.8 kw at 208V (the voltage used).
- The super-heater was connected to the boiler through 6.35 mm OD SS316 tubing. The super-heater was made with 25.4 mm OD SS316 tubing. It is 150 mm long and contains a cartridge heater inside. The heater is 19 mm in diameter and is 150 mm long. The rated power output is 500 w at 120V.
- The new injector is as described above (immediately following Figure 14).
- "Kaowool" blanket was used to insulate the boiler and super-heater. Heating tape was wrapped around the injector and used to help minimize heat loss.
- The injector fuel tube was water cooled and connected to a 3-way valve so that nitrogen flows through the fuel tube when the fuel feed is closed. The fuel tube contains a 60μm inline filter.
- As noted above, fuel and boiler make-up water flow-rates were measured with rotometers. Each rotometer was calibrated for the particular fluid using the "stopwatch and bucket" method.
- Steam flow-rate was calculated by using a choked orifice relation for the system back-pressure orifice. For this testing, a 0.57 mm diameter orifice was used and calibrated for 200 mg/s of steam and 35mg/s of diesel vapor at 650 kPa (79.6psig) and 300°C.

Results:

- The injector testing was commenced when the injector temperature (measured at the cell attached to exit of the injector, shown in Figure 14) reached 250°C. The injector temperature ultimately stabilized at 265°C in this

testing. The boiler pressure was 82 psig; and the injector pressure was 76 psig. Steam temperature going into the injector was 410°C; and the diesel flow-rate was 35mg/s. The injector testing lasted for 1hour and the conditions remained stable throughout the testing.

- The steam/diesel mixture stream exiting the system backpressure orifice appeared as a jet of very fine aerosol.
- A 5 mw He-Ne laser beam (red) was directed across the mixture stream. Visually, the intensity of scattering appeared uniform across the stream. Bright bursts of scattered light from droplets of diesel were never observed. The laser light did not visibly scatter from an exit stream of pure steam.
- After the testing, the injector was cooled down and disassembled for inspection. There are traces of diesel in the steam plenum and vaporizing tube but no evidence of coking in those parts was noted.
- The ruby tip, used to provide the jet of liquid diesel at the exit of the fuel tube, was coated with black residue. This could be from coking of the diesel fuel. Small amounts of diesel fuel left on the ruby tip from the diesel-to-nitrogen switching maneuver, or from dribbling, might not have been entrained by the steam and thus could have undergone coking.

Exploring the exit jet of the system

A fine mist was consistently observed in the diesel-vapor-steam jet issuing from the backpressure orifice at the exit of the injector. It was suggested that the mist might be caused by condensation of diesel vapor as the jet rapidly mixed with the cool ambient air. A number of tests were performed to verify this mechanism of mist (aerosol) formation. Close observation showed the mist forming a few millimeters (5-10) downstream of the exit of the backpressure orifice. No scattering from the He-Ne laser beam passed through the jet is seen in the clear region. When glass tubing was placed around the jet (so that the jet did not come in contact with the ambient air), no visible mist formed within the glass tubing. There is no visible He-Ne laser beam scattering from the jet inside the glass tubing. It was concluded the mist indeed forms outside the injector – the mist did not form within the injector as a result of incomplete vaporization or condensation.

Production testing

A larger vaporizing tube was built, bringing the injector to the final design used, as described above following Figure 14. Highest steam temperatures (480-550°C) possible with the experimental rig were explored. The nominal flow rates of the new testing were 55 mg/s diesel fuel and 215 mg/s steam. The new vaporizing tube gave about 85ms of residence time for the new flow rate. Following are the summaries of the testing.

Test settings:

- The backpressure orifice was bored to 0.660mm (#71 drill), which permitted a flow 215mg/s of steam and 55mg/s of diesel vapor at 300°C and 75psig.
  - The discharge coefficient of the backpressure orifice was evaluated by an experiment; the discharge coefficient was 0.6.
  - The boiler pressure and the injector pressure were kept at about 80 psig and 75 psig, respectively.
  - The temperature at the measurement cell, was maintained at a temperature of 300-315C.
  - The duration of each test was 2 hours.

After each test the rig was cooled down, and the injector parts were inspected for coking. Following are the observation of the parts after each run:

- The inside wall of the vaporizing tube was clean of coke. Evidence for coking was tested by running a cotton swab through the vaporizing tube. A small amount of raw diesel (by traces of red material) was picked up on the swab, along with very small traces of brown material. The small amount of diesel fuel was probably caused by the purging of the injector by cold nitrogen when the fuel was shut off. (The nitrogen purged the fuel line and injector until the rig is totally cooled down.)

- A small ring of carbon was found around the exit of the atomizing nozzle. As the steam/diesel passes through the nozzle and expands in the vaporizing tube, the boundary layer of the steam/diesel jet separates and recirculates toward the nozzle block containing the orifice. Unvaporized diesel droplets or diesel vapor could be entrained by the recirculating flow and cause coke to form on the exit side of hot nozzle block.

In one of the tests, coke was found on the atomizing nozzle block. The diameter of the nozzle was reduced by this coke. There was no noticeable difference in the testing conditions except the superheated steam temperature was 550°C, whereas the previous testing had been conducted with 480°C superheated steam temperature. A series of three tests was performed to investigate the formation of coke. Following are the summaries of the investigation:

- Test 1: Mixing of diesel and steam was started when the superheated steam temperature reached about 400°C and continued at this temperature for 90 minutes.
- Test 2: Mixing was started when the superheated steam temperature reached 400°C and continued as the steam temperature was increased to 550°C. Testing lasted 115 minutes.
- Test 3: Mixing was started when the superheated steam temperature reached 550°C and continued at this temperature for 120 minutes.

The nozzle block was observed with a microscope and no coke was seen affecting the nozzle of the atomizing nozzle block. Thus, the coke observed in

the earlier test was not replicated. However, there was a small ring of carbon deposit around the nozzle on the downstream face of the nozzle block. This appears to be a general occurrence – the recirculation zone downstream of the nozzle block causes a small build up of carbon on the backside face of the nozzle block. Next, long-term tests were conducted to further study the carbon problem.

The diesel-steam injector was tested for 16 hours over two days based on the following nominal conditions:

- Steam flow of 215 mg/s.
- Diesel flow of 55 mg/s.
- Temperature at outlet of injector tube set for 300 degrees C. This required a steam inlet temperature of 450 degrees C.
- Pressure at outlet of injector set for 75 psig.

The injector was tested for 8 hours, shut down overnight, and then run for another 8 hours on the second day. After the 16 hours of testing, the injector was allowed to cool and then was opened up and inspected.

The injector performed flawlessly throughout the 16 hours of testing. Upon inspection of the injector, some small amounts of carbon were noted:

- A light deposit of carbon was found on the downstream face of the atomizer nozzle block.
- A light deposit of carbon was also found on the inside of the vaporizing tube immediately downstream of the nozzle block.
- The deposits were light and did not plug the injector.

These light deposits of carbon are associated with the recirculation zone that sets up behind the atomizer nozzle block, as the steam-diesel jet expands into the injector tube. It may be possible to eliminate the carbon deposition by designing and fabricating an injector vaporizing tube with a tapered front end. This would maintain streaming (without recirculation) of the steam-diesel flow.

Also observed was the deposition of a light coating of carbon on the thermocouple placed in the flow in the measurement cell at the end of the injector. The temperature of the thermocouple is about 300 degrees C. Behind the thermocouple, a small recirculation zone is set up. Tube fittings in the test section also collected some light deposits of carbon.

The observations of carbon indicate the stream of steam mixed with the vaporized diesel fuel carries a small amount of aerosol carbon. A light deposition of carbon occurs when the mixture dwells for a while in a recirculation zone.

Questions remaining are the following:

1) Will the carbon deposition become a problem in practical application of the injector over hundreds of hours and over many startup-shutdown cycles?

2) Is equilibrium reached between the deposition and removable of the carbon, leading to small, insignificant steady-state deposits?

Subsequent testing of the injector nine months later, following the laser Rayleigh scattering measurements described in next two sections of this report, did not show carbon. The reasons for this difference relative to the earlier test results are unclear. It may be that the injector was operated on the borderline of carbon formation, and that small changes in operating conditions or fuel quality trigger the formation and deposition of small amounts of carbon. At the end of this report a section is provided reviewing the formation of carbon in steam hydrocarbon reformers and in steam-diesel mixtures.

LASER SYSTEM

The laser system for diagnosing the completeness of vaporization and mixing at the outlet of the injector was set up and tested. The laser Rayleigh scattering (LRS) method is used since it permits the degree of mixedness of the diesel vapor with the steam to be readily discerned. This is possible because the scattering cross-sections of steam and diesel vapor are very different. Steam weakly scatters the laser light, diesel vapor strongly scatters the light, and diesel-steam homogeneously mixed at the desired mass ratio scatters the laser light with an intermediate intensity. Thus, by measuring the rms fluctuation of the scattered light, and comparing it to the mean signal, it is possible to ascertain how well the injector has mixed the diesel fuel into the steam. Some previous uses of scattering methods applied to jets are given by Yee (1982), Cavaliere et al. (1988), and Espey and Dec (1997).

The laser optical system is depicted in Figure 18. The main elements of the system are as follows:

- Argon ion laser (Coherent Innova Model #308), giving nominally 1 watt of continuous power for the 514.5 nm line. Beam diameter is about 1.8 mm. The electrical requirements of the laser are: 240 volts 3-phase, 55 amps per phase maximum power.
- A water chiller (220 volts AC, 10 amps) is used in the water-cooling loop of the laser.
- Collection optics for gathering the light scattered from the laser beam at 90 degrees normal to the laser beam. The solid angle of the collected light is about 0.1 sterradian. The scattered light is measured with a 1P28 photomultiplier tube. A drawing of the collection optics system is shown in Figure 19. The optical parts are list as follows:
    - x2 spherical lenses, 50.8 mm diameter, BFL = 67.43mm
    - x1 spherical lens, 12.7 mm diameter, BFL = 15.48mm
    - x1 narrow-bandpass filter with peak transmission at 514.5nm
    - x1 1mm slit
    - x3 1-axis stages for mounting the lenses and slit
    - x3 3-pronged lens holders.
    - Fabricated enclosure made of 12.7 mm and 6.35 mm aluminum sheet, inside faces painted flat black
- Laser beam dump.
- Signal display processing is done with a digital oscilloscope (Fluke Combiscope).

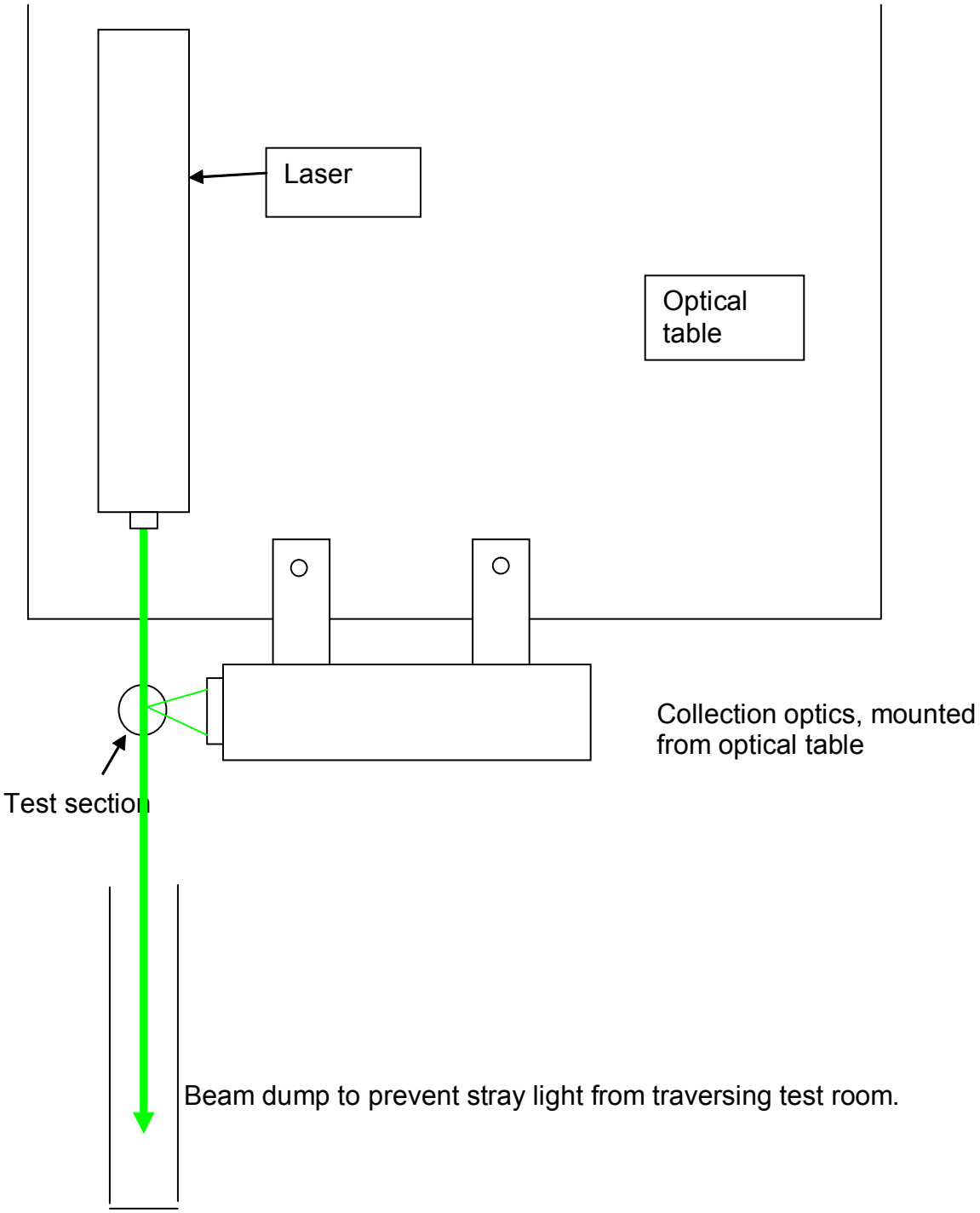

Figure 18: Laser optical system, viewed from top

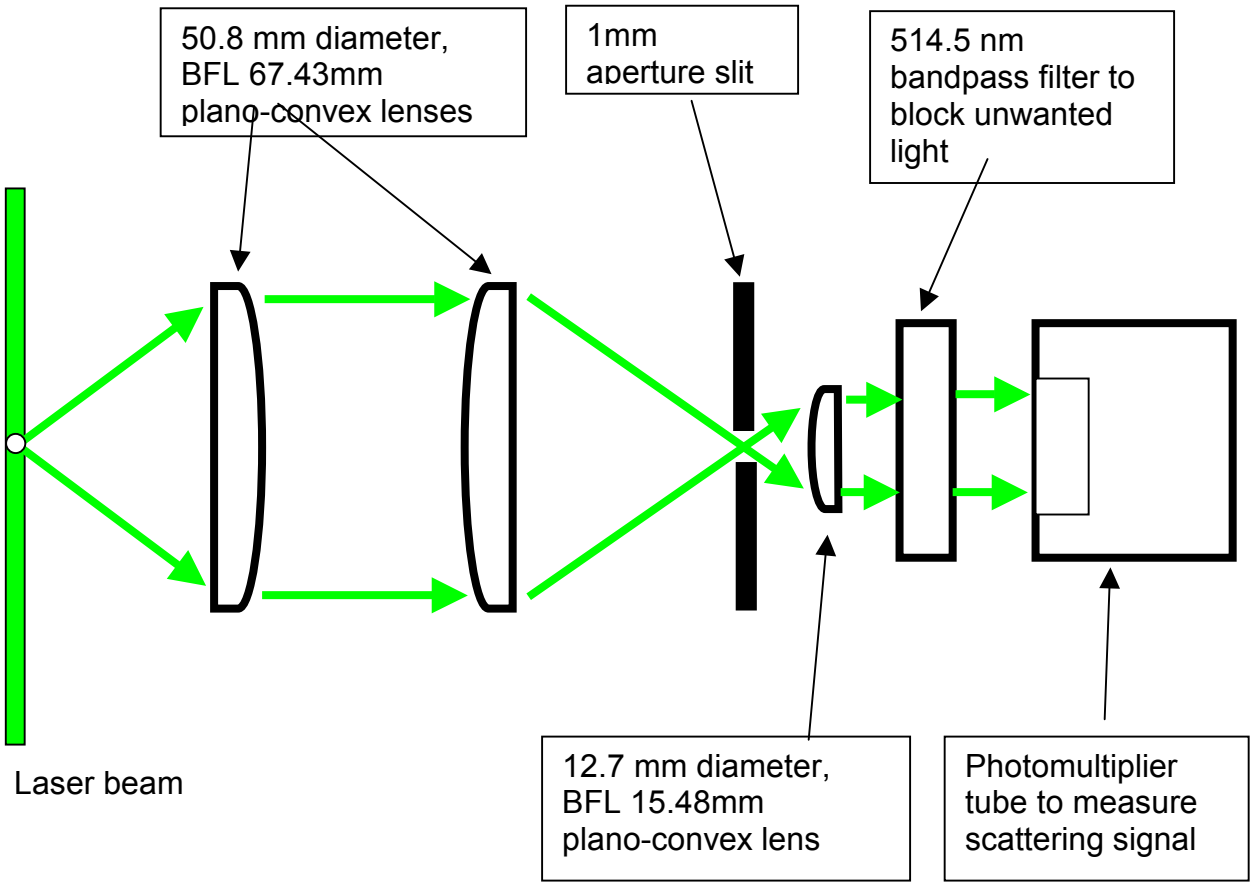

Figure 19: Collection optics

Debugging experiment

Experience with the laser system and the LRS method was obtained, and debugging of the system was performed, by examining the scattering from several gases. Scattering signals from helium, nitrogen, and ambient air were measured. The laser-optical system readily distinguished between He and N_2 in the measuring section. The test volume examined was about 1 mm^3 Tests performed included:

1. Gas scattering – the gas of interest was flowed through all passages of the coaxial jet system, or with no flow, ambient laboratory air was present.
2. Concentric jet scattering contours were measured in order to test the LRS method's ability to distinguish the scattered light signal from small volume.

The jet system used for the experiments is a coaxial jet, mounted on a 1-axis translator. The inner jet was made of 6.35 mm o.d. stainless steel tubing, while the outer tube was made of pipe of about 20.5 mm i.d.. The tube and pipe were silver soldered into a manifold that accepts two gas inputs for the inner and outer jets. Within the outer pipe there is a set of six perforated plate disks that even-

out the flow from the manifold to help produce a uniform flow. Figure 20 depicts the concentric jet setup and relevant measurement points.

A 1-axis translator allows for movement of the coaxial jet system through the measuring volume defined by the laser beam and collection optics, which are fixed. This movement gives the scattering contours across the jet system. The following data include tests used bottled gases, for which no outside air entered the measuring volume, as well as contour tests in which the scattering signals were measured as a function of radial distance from the center of the jet assembly.

Gas Tests

This set of tests was performed with the gas of interest flowing through all passages (jets) of the coaxial jet system, or with ambient laboratory present. The measurements were made on the centerline of the jet system 2mm above the exit of the jet system. PM tube voltage was set at 1000 volts dc.

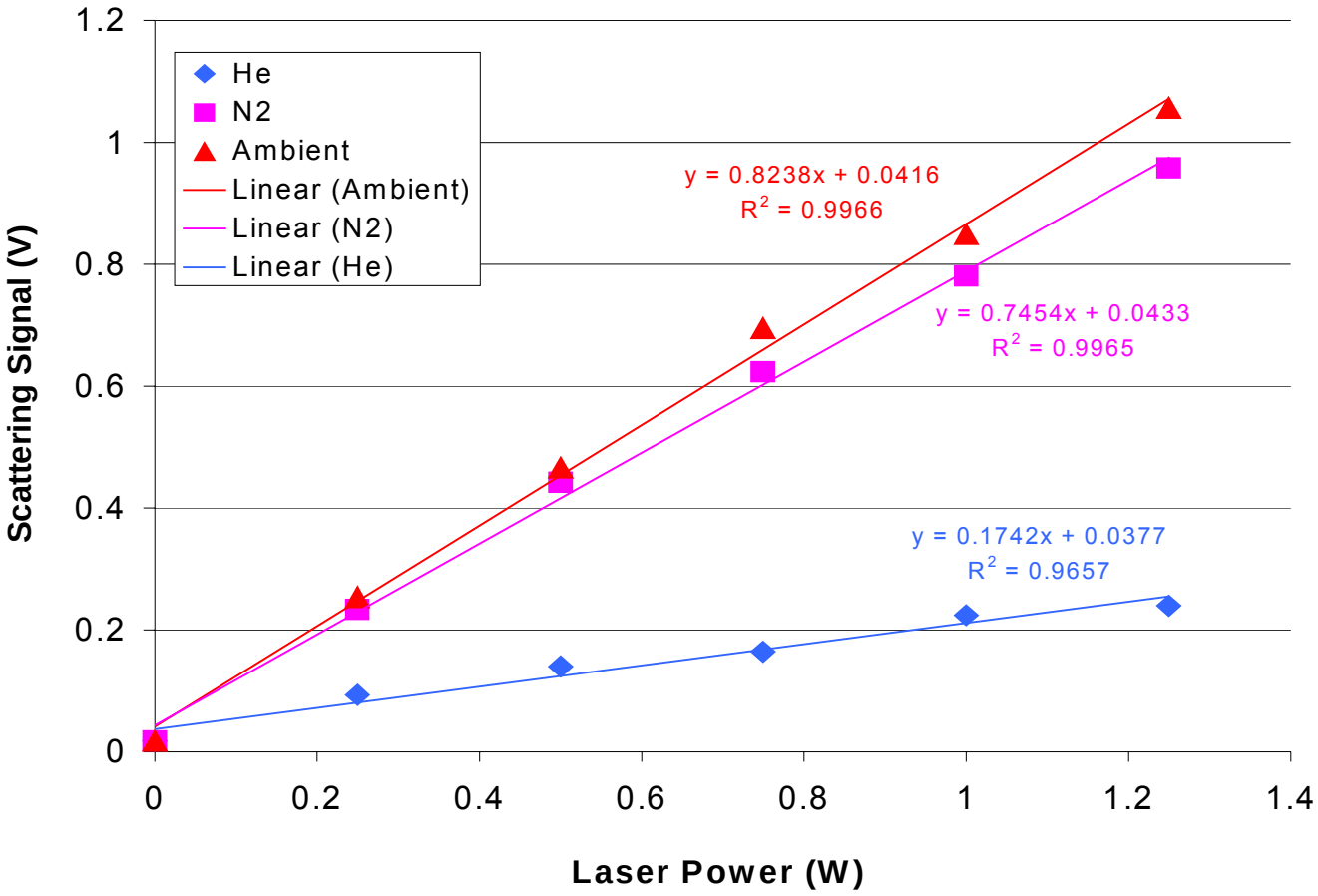

Figure 20: Scattering signal from gases versus laser power

Figure 20 depicts the time-mean scattering signal versus laser power. Six data points were taken for each gas (including the zero laser power point) and linear regression lines were fitted using spreadsheet software. For the tests with bottled N_2 or He following through the jet system, ambient laboratory air was eliminated from the test volume.

Figure 20 shows the time-mean scattering signals for three different gases. The ambient air and N_2 are relatively close in scattering signal, which is expected, with air having a slightly higher average signal due to particles in the air that scatter heavily. Helium is well below N_2, which is also expected, and is readily distinguishable from N_2 by the collection optics.

Figure 21 below shows similar data taken during a different test. The laser power is now constant for each gas, and the standard deviation is compared with the time-mean scattering signal.

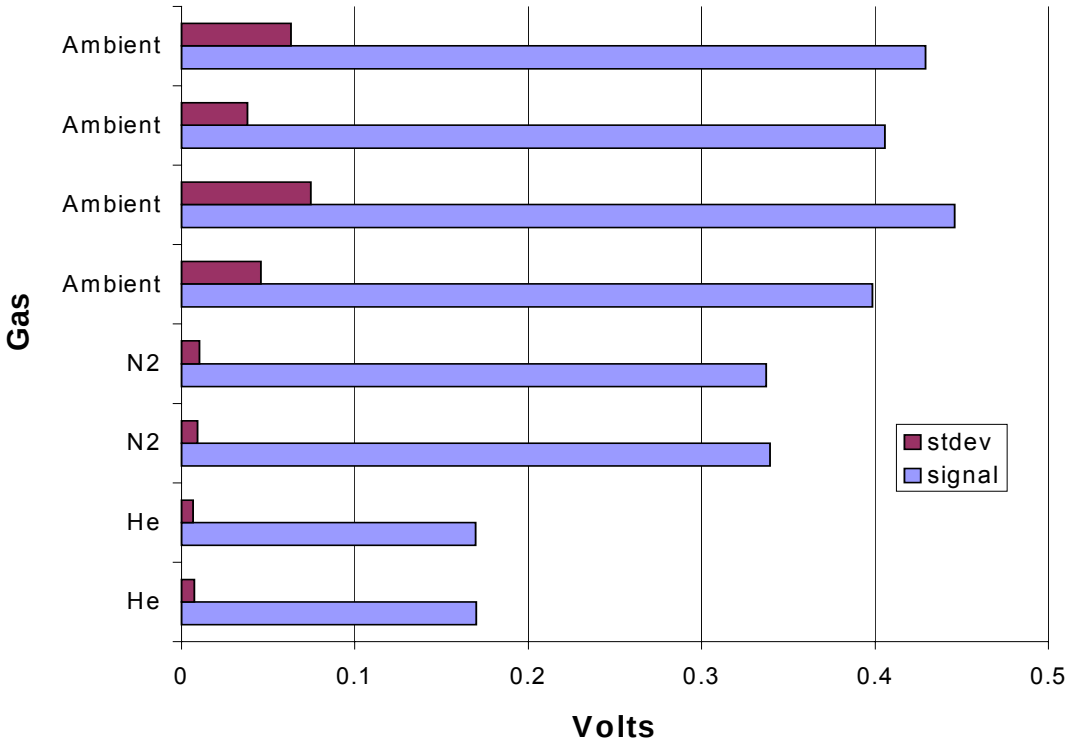

Figure 21: Comparison of standard deviation (purple) with time-mean scattering (blue) from ambient laboratory air and from jets of N_2 and He.

As noted in Figure 21, the standard deviation in the scattering signal of air is much greater than for the bottled gases (N_2 and He), because of the particles in the ambient laboratory air.

Figure 21 shows repeatability in the measurements for the pure gases. The signal for the bottled gases does not change over time, and the standard deviation-to-mean ratio is much less than one.

Contour tests

This set of tests was run with He flowing in the inner jet, and N_2 flowing in the outer jet. The exact gas flow-rates have little effect on the scattering signal, since for the conditions used there is little aerodynamic compressibility effect. The flow-rates do, however, influence the mixing and concentration profiles downstream of the jet system exit. The following data were taken roughly 2 mm above the jet, where the potential core of He should still be intact. Figure 22 shows the scattering signal versus radial position for the He-N_2 concentric jets. Figure 23 shows a similar test, taken on a different day.

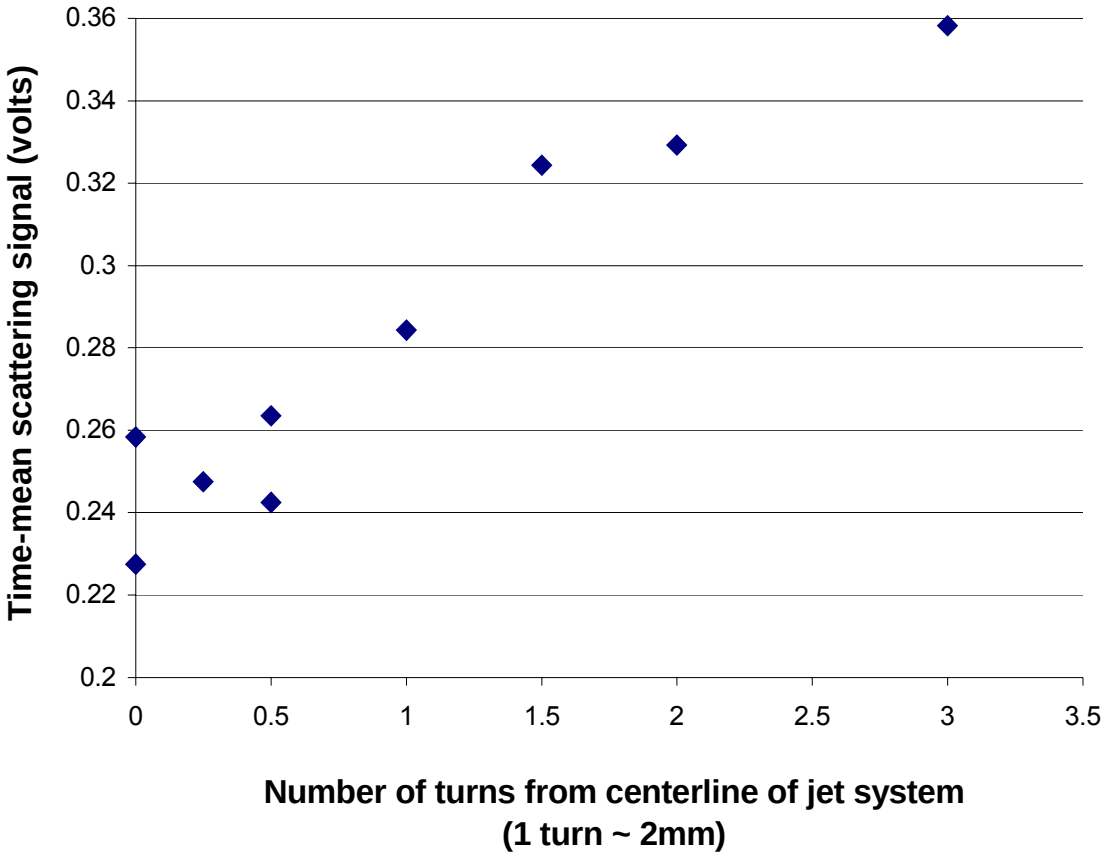

Figure 22: Time-mean scattering signal versus radial position in He-N_2 coaxial jet

Figures 22 and 23 show the scattering profile along the coaxial jet radius. Note the low scattering in the He region (center) and the gradual rise as the measuring volume is moved radially outward into the N_2 region. The inner He jet extends to about 1.5 turns (~3 mm).

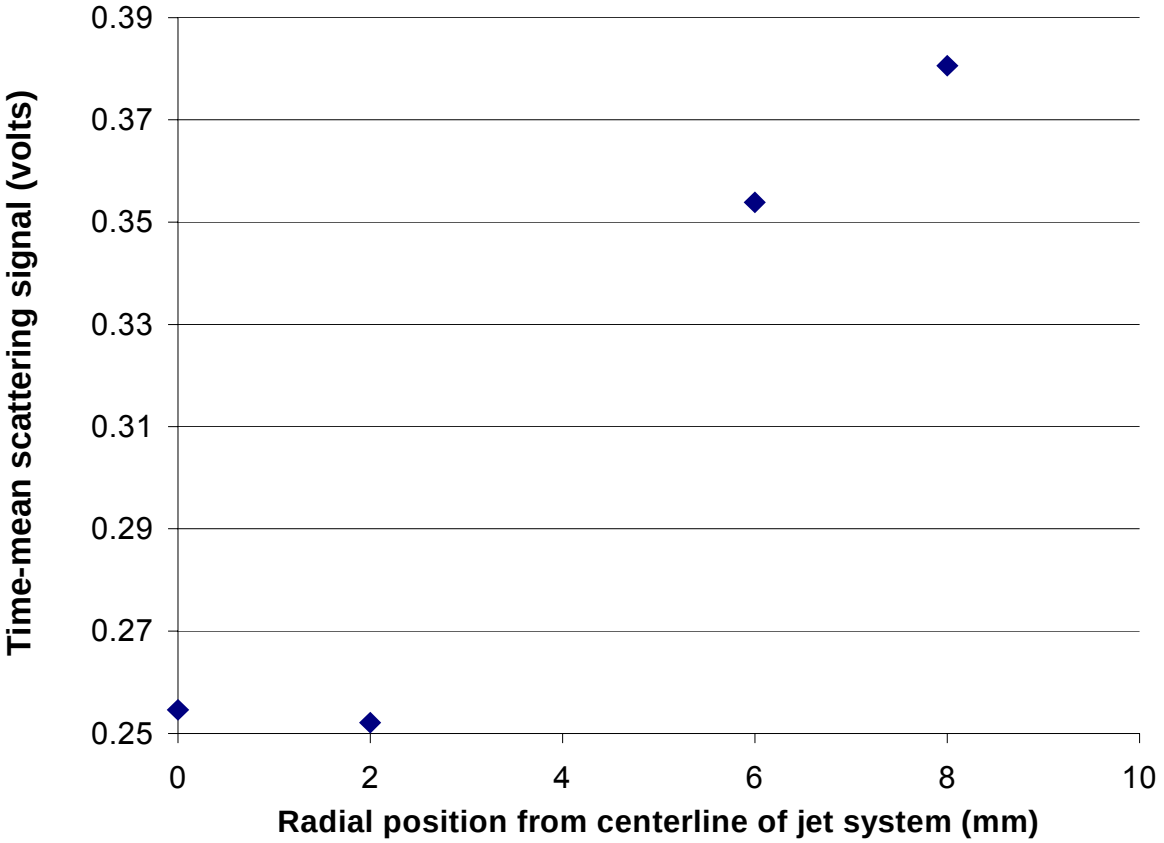

Figure 23: Time-mean scattering signal versus radial position in He-N_2 coaxial jet

Additional gas tests

Additional gas scattering measurements were conducted by including methane (CH_4) and hydrogen (H_2) in the group of gases tested. Table 1 below gives calculated scattering ratios for gases relative to N_2 at room temperature and 1 atm. Liquid fuel vapors, such as diesel fuel vapor, scatter much more heavily than N_2 or H_2O, as the refractive index generally increases with fuel carbon content.)

Figure 24 below shows the measured scattering signal versus laser power for jets of the gas, including CH_4, N_2, H_2, and He.

TABLE 1

Scattering cross sections of various gases and comparison to N_2.

Gas	scattering cross section	σ_{N2}/σ_{gas}
N2	7.0525E-28	1
CH4	1.5433E-27	0.4570
O2	5.8004E-28	1.2159
H2O	5.0248E-28	1.4035
H2	1.5280E-28	4.6155
He	9.5679E-30	73.7095

The scattering signals for He and N_2 in Figure 24 agree with results presented in Figure 20, and the order of the scattering varies with gas type as indicated in Table 1: [Table 1 is based on calculations of Rayleigh scattering by gases using the data of Gardiner et al. (1981).] However, the measured ratios of scattering relative to that for N_2, do not agree with the values in Table 1. Several fixes were attempted to increase the scattering ratios – especially for N_2 compared to H_2 and He. It was found that the collection system was catching scattering from the laser beam at the edges of the jet. This led to a systematic offset of the scattering signal for low-scattering gases such as H_2 and He. Blinds were installed around the 1mm slit in the collection system, so that only the light passing through the slit could possibly reach the PM tube. This changed the scattering signals, increasing the scattering ratio between N_2 and H_2 from about 2.5 (in Figure 24) to about 4.5, a value agrees with the calculated value of scattering ratio. Also, the He scattering signal became much lower than shown in the figures above, and the N_2/He ratio approached the 73 value of Table 1.

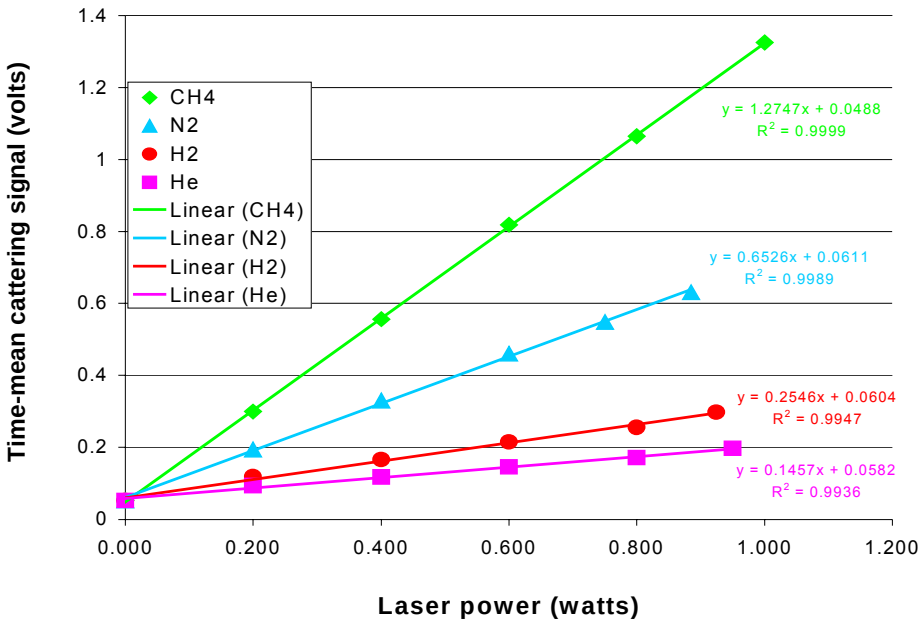

Figure 24: Time-mean scattering signal versus laser power for gases

LASER RAYLEIGH SCATTERING MEASUREMENTS

The outlet stream of the injector for the 1000 watts fuel cell was tested by the laser Rayleigh scattering method. This testing was performed with the injector operating at atmospheric pressure. Outlet temperature was varied up to approximately 500 degrees C. The steam mass flow was held constant, while the diesel mass flow was varied over a considerable range. Typically, the ratio of the rms to the mean of the scattering signal was 0.1, indicating an acceptable mixedness of the diesel vapor with the steam. No evidence of carbon formation was found during these tests.

The nominal conditions used are listed as follows:

Boiler T ----------	163 °C
Boiler P ----------	80 psig
Super-Heater T ----------	488 °C
Injector T ----------	500 °C
Steam Flow ----------	250 mg/s
Diesel Flow ----------	20 to 65 mg/s

The back pressure orifice was moved from the exit of the injector to a position downstream of the super-heater, upstream of the injector, so that the steam flow could be metered and brought to nearly atmospheric pressure for mixing with the diesel fuel in the injector. The steam flow-rate is based on a compressible flow equation, for choked flow through the orifice: $1.0695e\text{-}2*P_0/T^{0.5}$ [mg/s].

In order to maintain the injector at 500 degrees C nominal temperature, heating tape was used around the injector. For running at 500 degrees C, 1 atmosphere pressure, the residence time of the gas in the injector's vaporizing tube was about 10 ms. The injector was place upright, with the exit stream jetting vertically up. The laser beam and collection optics were located about 1.5mm above the exit of the injector vaporizing tube. Outside should not have been present in the measurement volume.

First series of tests

The results presented below represent several days of testing – the laser Rayleigh scattering measurements were repeatable from day to day. The scattering signal was read on the oscilloscope in real time, and data "snapshots" were taken at the operator's discretion. Also note the time traces of scattering signal are negative; ie, the stronger the scattering the more negative the signal. Zero signal corresponds to no laser scattering.

Several sets of data were taken with steam and a small amount of helium purging the diesel feed tube. Aligning the collection optics with the steam jet was relatively easy, since the ambient air was somewhat dusty and sharp peaks (Mie scattering) were noticeable on the oscilloscope. The steam, derived from distilled water, was clean and no sharp peaks were noticed. The steam signal

was steady and flat, characteristic of totally vaporized (superheated), clean steam. The baseline steam signal was roughly 20 mV on the oscilloscope.

When diesel fuel was introduced, a temporary sputtering was observed both audibly and on the oscilloscope. Figure 25 shows a typical reading during the initial sputtering phase. Note that when a droplet was present, the scattering signal went off-scale. The measurements near zero volts represent steam, while the negative measurements indicate the presence of diesel fuel.

Figure 26 displays scattering signal time traces for several diesel flow rates. The steam flow rate was constant. Sputtering was observed at lowest diesel flow rate. As the diesel flow rate was increased, the sputtering disappeared and the scattering signal became stronger as more diesel fuel was added, which is expected.

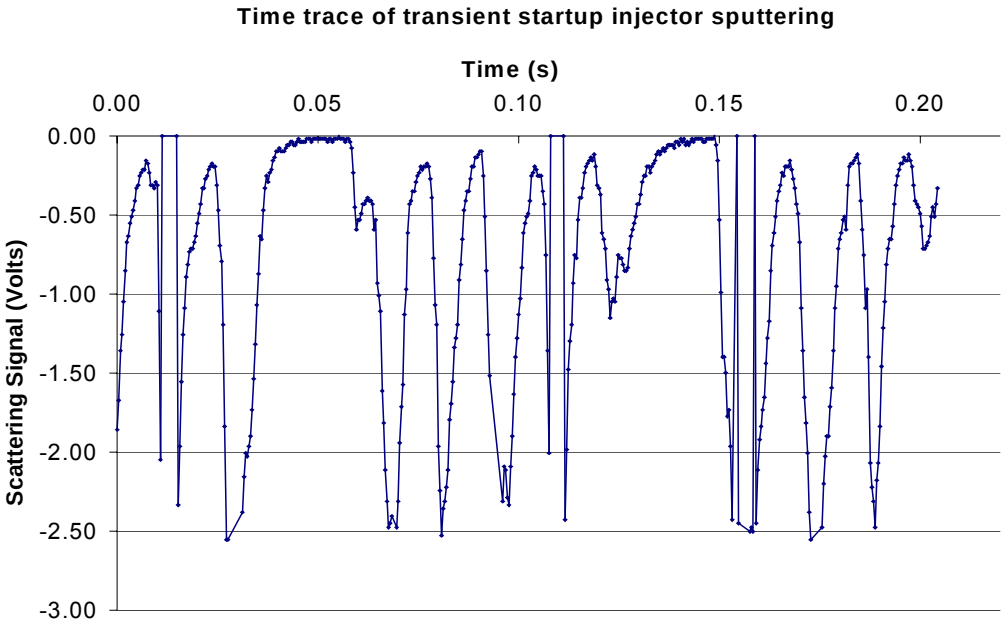

Figure 25: Temporary sputtering of injector when fuel is introduced. Note the clear distinction between steam (0 volts) and diesel (as low as -2.50 volts).

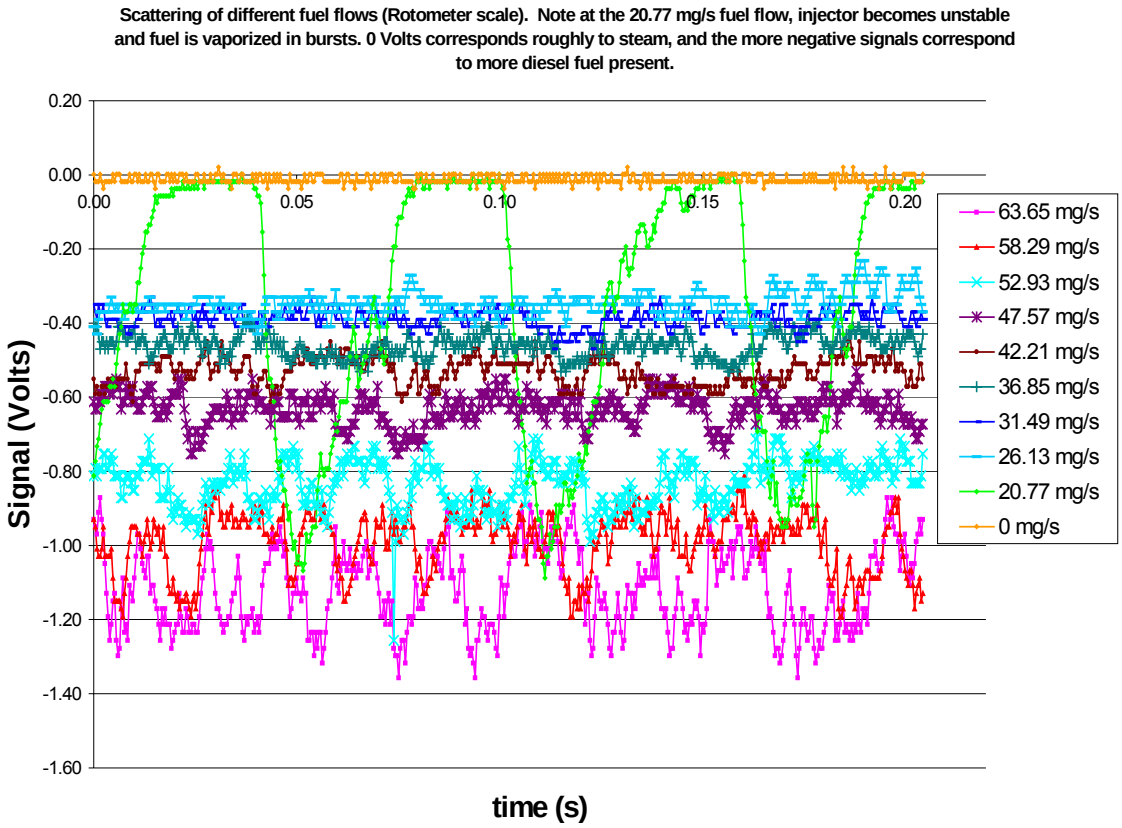

Figure 26: Time traces of scattering for various fuel flow rates. Note the stronger scattering signal corresponding to higher diesel fuel concentration. The light green trace contains injector instability at low fuel flow rate.

Figures 25 and 26 display time traces taken directly from the oscilloscope, which was in communication with a computer that stored the data). Data points are taken roughly every 0.4 milliseconds (512 points taken for 0.20 seconds). This time scale resolution was deemed optimal; smaller time intervals did not reveal any new information, and larger time intervals tended to obscure some of the "structure" visible in the signals.

Figures 27 and 28 (below) show reduced data. Figure 27 displays the time-mean scattering signal versus the diesel flow rate. The mean signal should increase with fuel flow rate for two reasons; higher diesel concentration and lower injector temperature from vaporization which increases the number density. The increase is observed in Figure 28. The mean signal appears to level out at the lower fuel flow rates. This region represents unstable operation, however, with the possibility of Mie scattering from diesel droplets impacting the signal.

Figure 29 shows a plot of the ratio of the standard deviation over the mean scattering signal versus the fuel/steam mass flow ratio. The standard deviation/mean scattering signal ratio is used as the indicator of diesel-steam

mixedness. The lower the standard deviation/mean ratio, the more well mixed the system; the higher the ratio, the larger the fluctuations relative to the mean. The mixing appears to improve with increasing fuel flow rate, reaching an apparently best condition when the diesel/steam mass flow ratio is about 0.15. Here, the standard deviation is roughly 7% the mean signal. This value is close to ratio of standard deviation over mean observed in the scattering signals from the jets of bottled gas, of about 5% (see Figure 21).

Figure 29 displays several traces taken at a fixed operating condition, at several spatial locations across the exit jet of the injector. The spatial differences in the scattering signal are small. The spread in the mean scattering signal is 3%, and the spread in the standard deviation (signal fluctuation) is about 8%. The signal is essentially independent of the position in the jet. Figure 29 contains two traces taken at the edges of the jet, and two traces taken in the center of the jet.

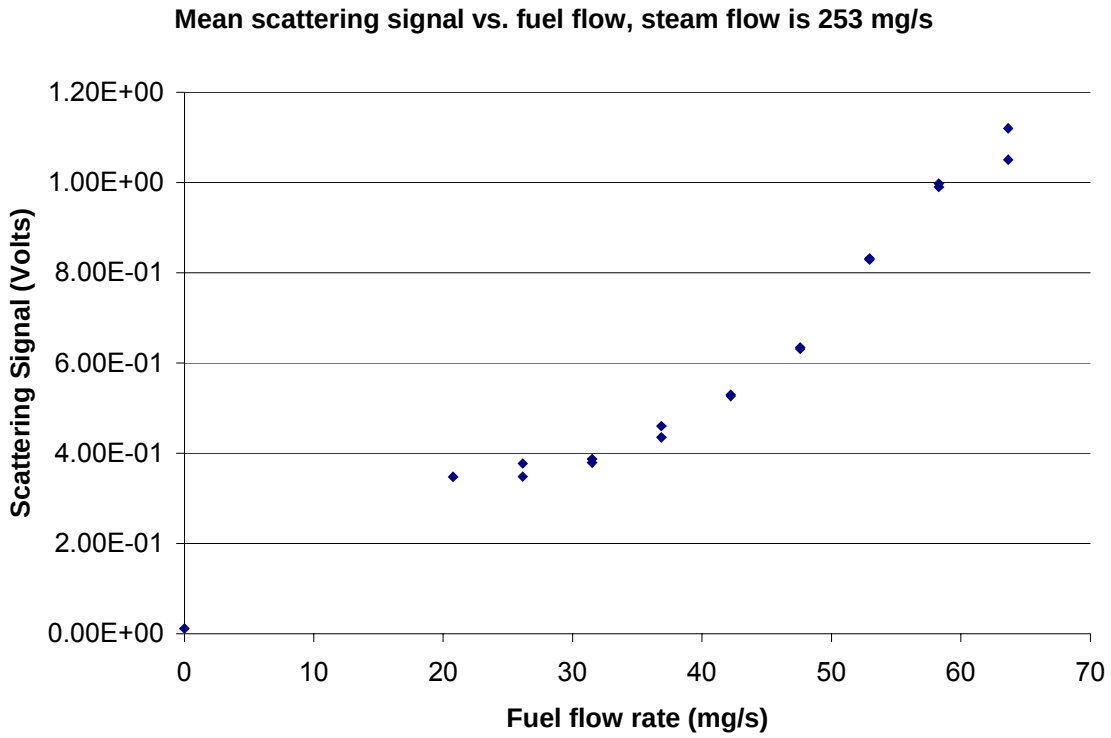

Figure 27: Time-mean scattering signal as a function of diesel flow rate.

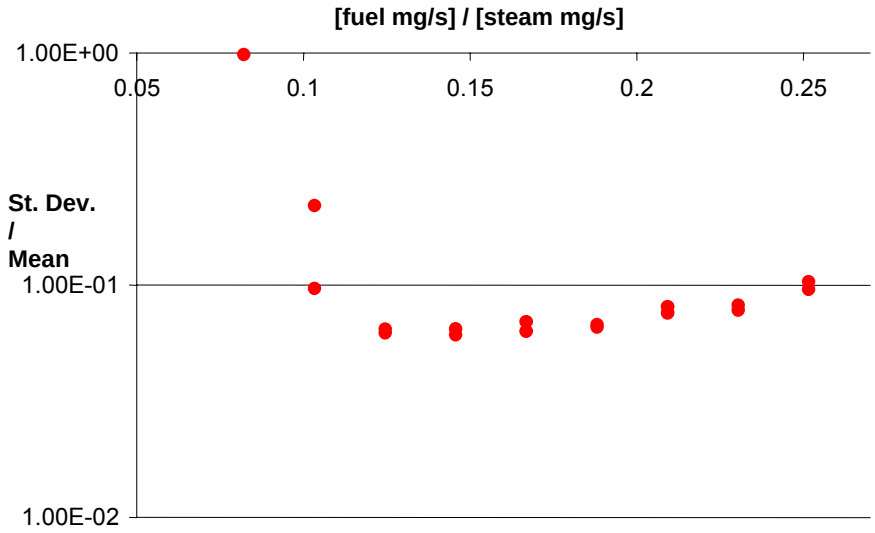

Figure 28: Standard deviation over mean of scattering signal versus diesel/steam mass-flow ratio.

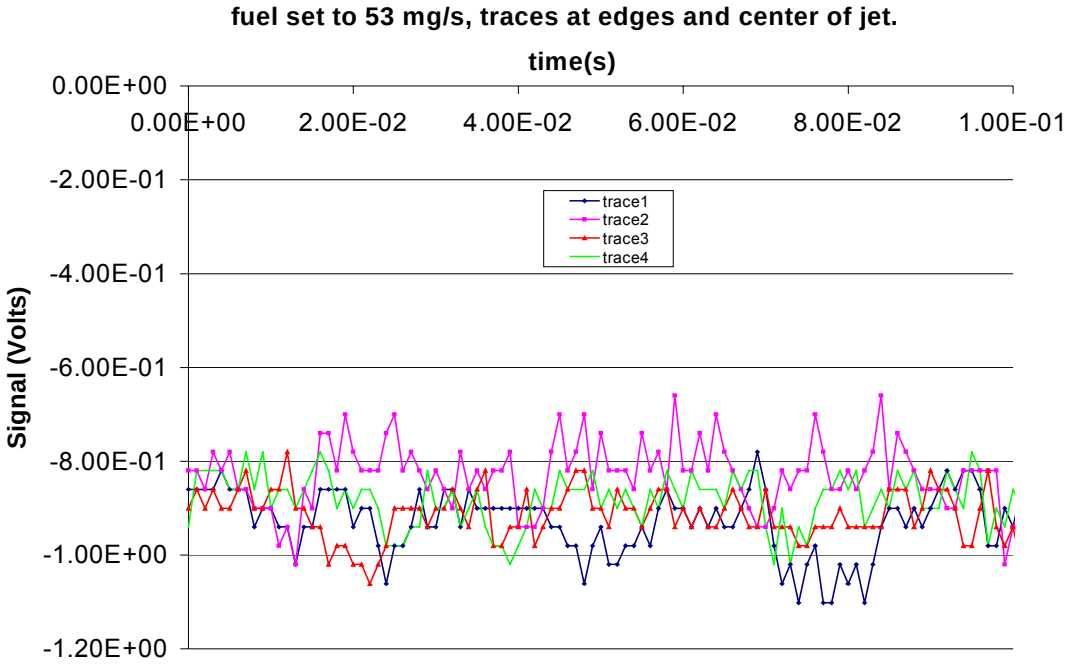

Figure 29: Time traces of scattering signal for several locations at injector exit

Second series of tests

The second series of tests on the laser Rayleigh scattering measurements of the injector complements, confirms, and adds to the first series of tests reported in the preceding pages. In these new tests, six steam flow rates (153 mg/s, 177 mg/s, 200 mg/s, 220 mg/s, 234 mg/s, and 259 mg/s) were examined. Normally, for each steam flow rate, eleven diesel flow rates were run (15 mg/s, 21 mg/s, 26 mg/s, 31 mg/s, 37 mg/s, 42 mg/s, 48 mg/s, 53 mg/s, 58 mg/s, 64 mg/s, and 69 mg/s). In addition to use of commercial number 2 diesel fuel, tests were also conducted with light naphtha.

The data presented in this section were obtained at atmospheric pressure in the injector vaporizing tube, with 133 mm of heated vaporizing tube length downstream of the atomizing nozzle. By using a heating tape wrapped around the vaporizing tube, it was possible to maintain a temperature of 500 degrees C in the vaporizing tube. The atomizing nozzle used for all tests is 0.79 mm in diameter, and the liquid nozzle is 150 microns in diameter. The optical measurement volume used for these tests is 2.5 mm^3. Data are presented in five groups: 1) diesel results which include data at various operating conditions, 2) naphtha results which include data at various operation conditions, 3) additional diesel injector tests, 4) testing of an injector designed by InnovaTek, Inc., which uses an uncooled fuel feed tube and a larger atomizing nozzle than used in the UW injector, and 5) concluding tests of the UW injector.

Diesel results: Figure 30 displays the standard deviation over mean of the laser scattering signal as a function of the fuel / steam mass flow-rate ratio for several steam flow rates. The standard deviation over mean is essentially flat at 6-7%, though sharp increases occur at low diesel flow rates. These increases are due to the sputtering noted in the preceding section. The sputtering was found to be caused by vapor lock, where the liquid fuel has sufficient residence time to boil inside the liquid feed tube, and the liquid injector spits out fuel in a periodic manner (at a frequency of 19 - 22 Hz). The vapor lock can be avoided by introducing cooling N_2, air, or water around the liquid fuel feed tube. When cooling is applied, the standard deviation over mean settles down to the level consistent with no vapor lock.

Figure 31 shows a plot similar to Figure 30, but emphasizing the effect of cooling. When cooling was applied, the standard deviation over mean falls in line with that for the high fuel flow cases, which do not suffer from vapor lock. Figure 32 shows two time traces from which the average data were taken. Note the oscillations without cooling, and the smoothing of the signal that occurs with cooling. This change in liquid fuel flow pattern is audible; the unstable cases produce a ragged sputtering sound, while the stable cases produce a smooth hiss. The time traces depicted in Figure 32 were taken at a fixed fuel flow-rate and fixed steam flow-rate. Note that at higher fuel flow rates, no cooling was used since vapor lock instabilities were not present.

Diesel fuel is relatively stable within the operating conditions tested. Cooling is needed only at the low fuel flow rates (15-31 mg/s). No coking or deposits were found on the injector tube, nozzle disk or liquid injector tip. No droplets or particles were seen with the laser scattering method during operation, which implies that vaporization was complete and carbon aerosol was not formed. Particles and droplets are usually seen as sharp, strong spikes in our scattering signal, driving the signal off-scale. This behavior was not noticed during operation. The exiting mixture was clear – condensation did not occur until after the measurement section, once the exit jet mixed with room air. When the laser beam encounters condensation, an off-scale signal is recorded and bright laser beam scatter is observed -- this usually occurs when the purge gas is introduced as the liquid fuel is being shut off.

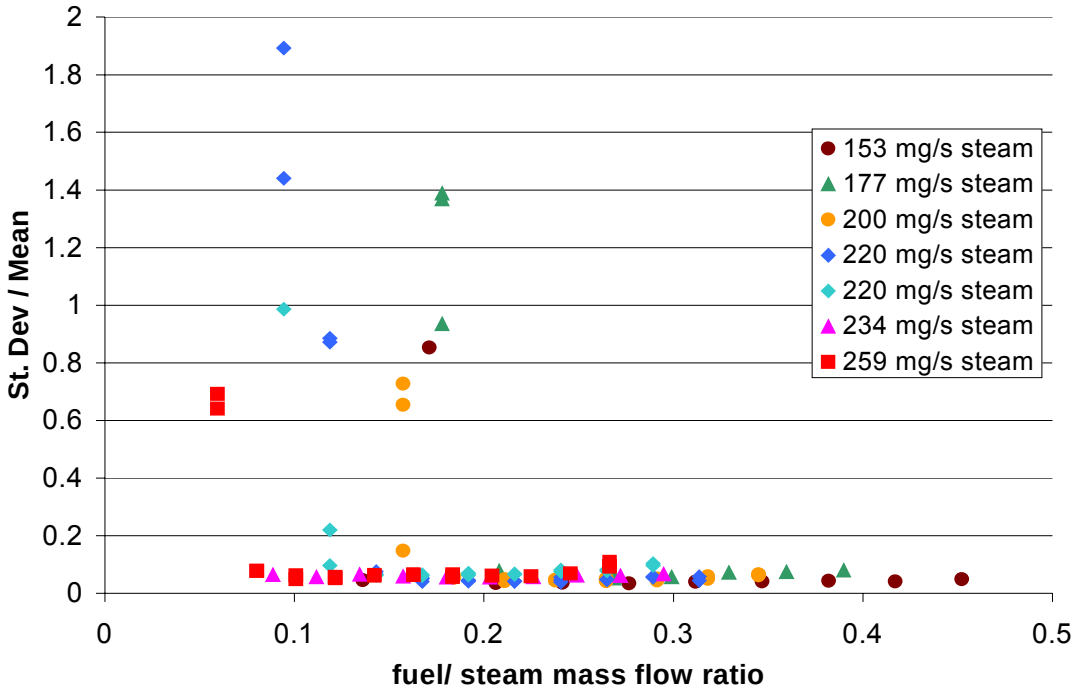

Figure 30: Standard deviation over mean of laser scattering signal as a function of fuel / steam mass flow ratio for several steam flow rates. No cooling of liquid feed tube.

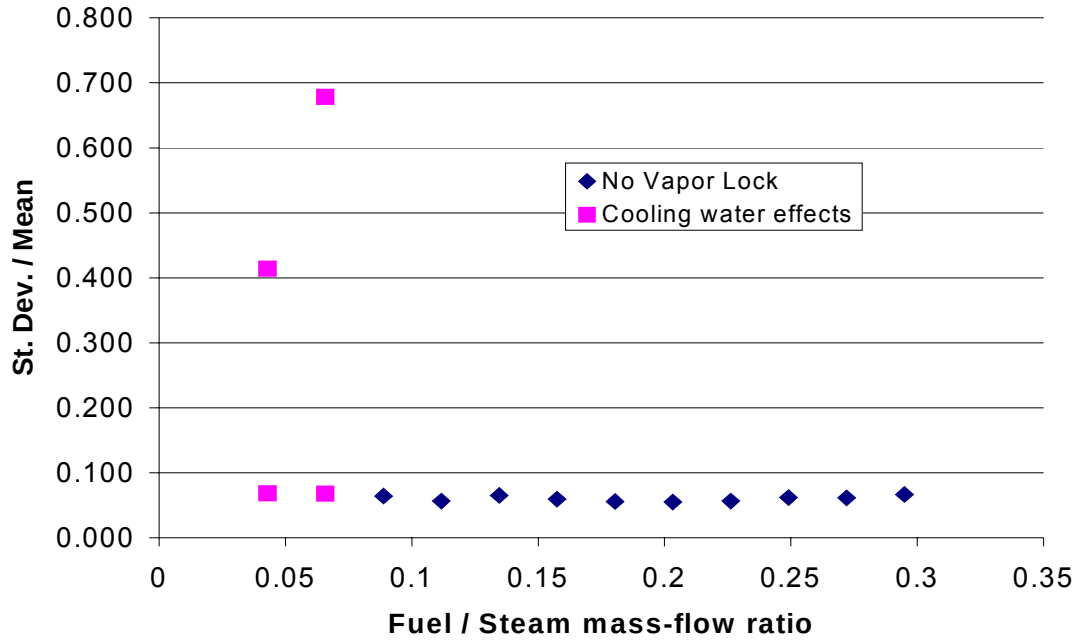

Figure 31: Effects of cooling on injector stability. Cooling water applied to control vapor lock for low diesel flow rates (squares). High diesel flow rate naturally controls vapor lock (diamonds).

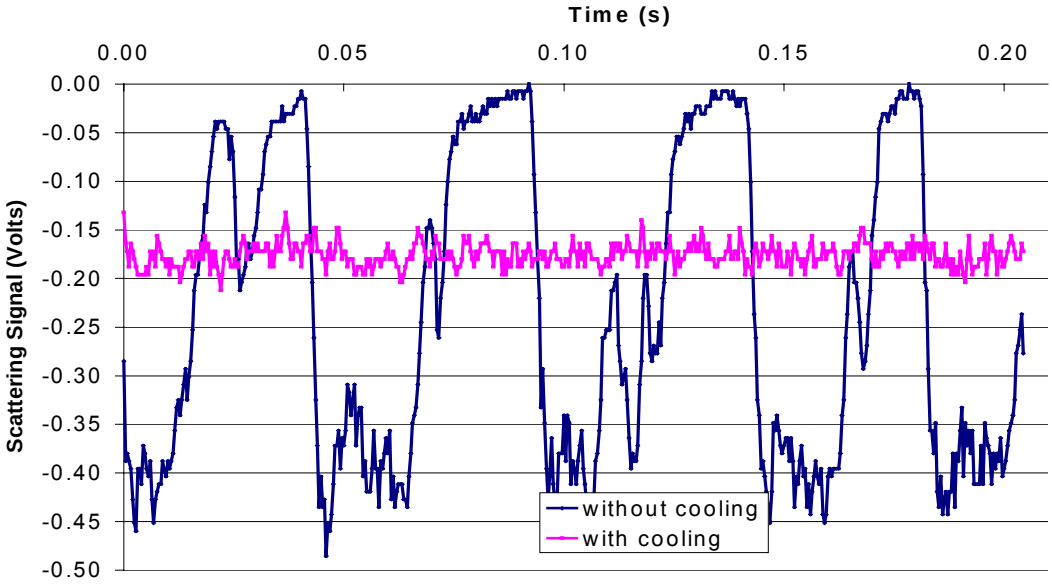

Figure 32: Time traces of scattering signal with and without liquid fuel cooling. Note the instability observed during vapor lock. Steam flow is 234 mg/s and fuel flow is 15 mg/s.

Naphtha tests: Light naphtha fuel was used for comparison with diesel fuel. Naphtha is a light distillate, significantly composed on cycloparaffins in the C_5 range, with a liquid density of about 710 kg/m^3, compared to diesel with a density of about 860 kg/m^3. The light naphtha used had a chemical composition of $C_{5.9}H_{12.45}$, while the diesel used was not analyzed but should be near the nominal composition of $C_{14}H_{26}$. This means that naphtha should scatter light noticeably less than diesel fuel, and thus produce a weaker signal. The experimental results did in fact follow this trend. Naphtha is more volatile than diesel fuel and more prone to vapor-lock. Experiments verified this: naphtha exhibited a narrow range of stable operation without cooling of the fuel feed tube. Figure 33 shows the standard deviation over mean in the laser scattering signal for various steam and fuel mass flow rates.

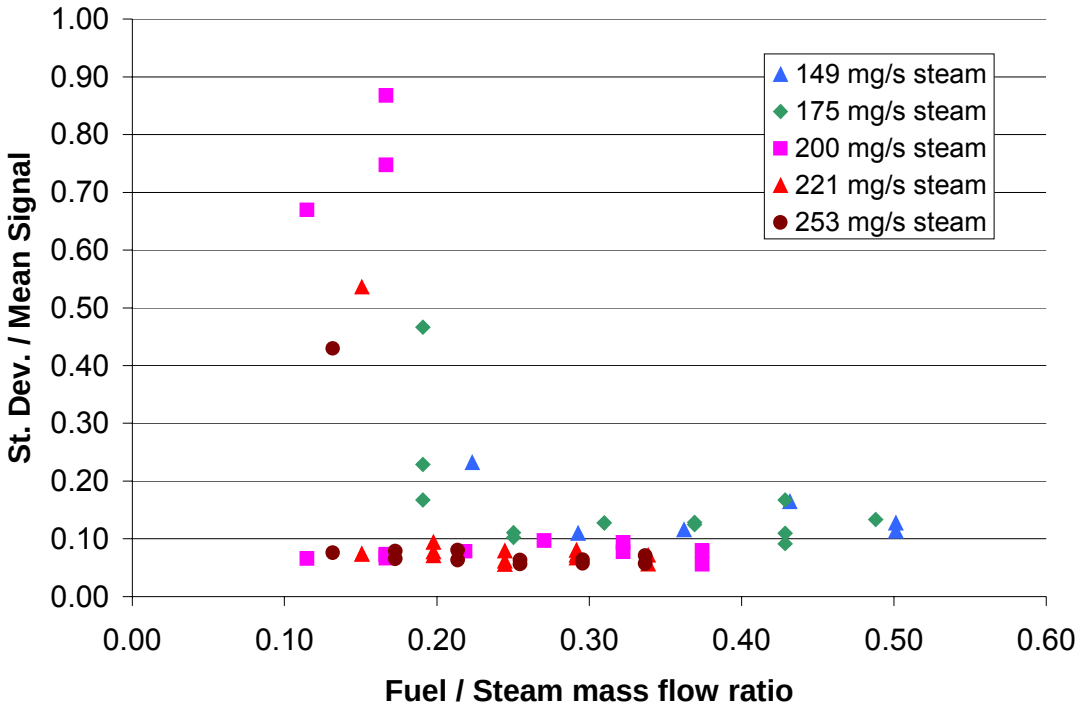

Figure 33: Laser scattering standard deviation over mean versus fuel/steam mass flow rate ratio for five steam flow rates. Light naphtha as the fuel.

The measurements for which vapor lock occurred (low mass flow ratio points with standard deviation / mean well above 10%) generally contain two points, with and without cooling. When cooling was introduced the vapor lock was partially suppressed, except at the two lowest steam flow rates. With the vapor lock suppressed, naphtha's standard deviation / mean was about 10%, which is about 50% greater than diesel fuel's 6-7 %. Although naphtha vaporizes more readily, its volatility encourages instability at the liquid injector tip, which produces larger

oscillations of concentration. During operation, the injector sounds more ragged on naphtha than diesel. If the exposed liquid fuel injector tip could be modified (by adding fine cooling passages), vapor lock would probably be less of a problem.

Additional diesel tests: Several additional tests were performed with diesel fuel and steam. The first test consisted of measuring the spatial variation in the scattering signal across the exit of the injector tube. Figure 34 depicts the mean signal, standard deviation and ratio of the standard deviation / mean for the vaporized tube outlet (7 mm id).

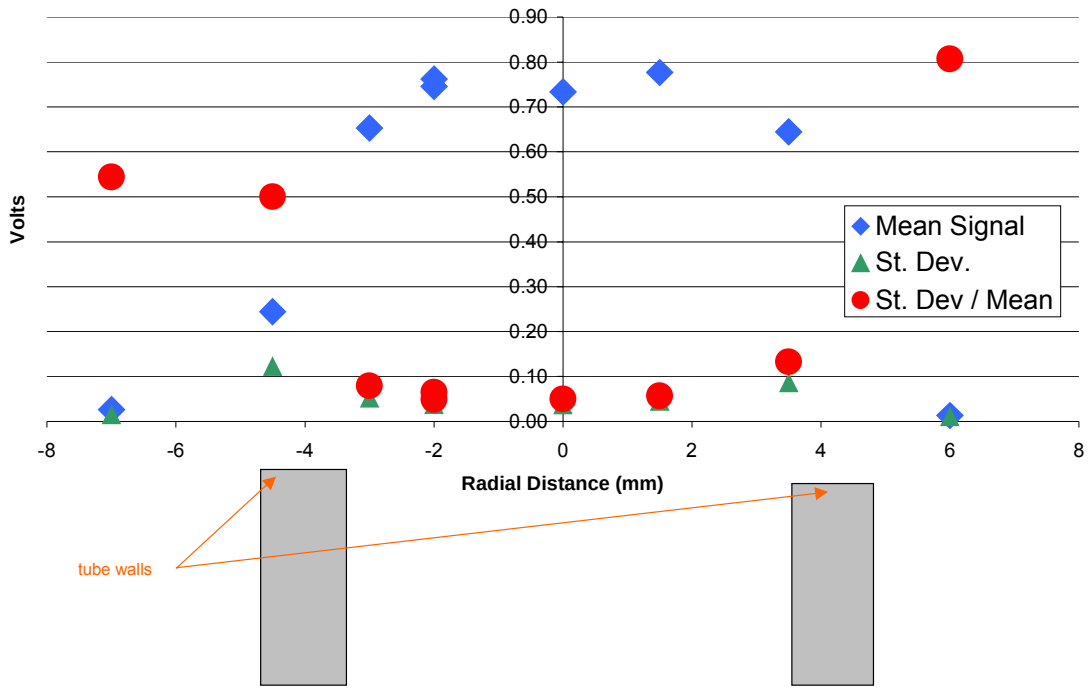

Figure 34: Spatial variation in scattering signal for the vaporizer tube outlet. The tube wall is shown, with the od being 9.5 mm and the id being 7mm.

The mean signal, standard deviation, and ratio are nearly constant across the exit stream of the injector, indicating good mixedness and uniformity of the steam with the diesel vapor exiting the injector tube. At the edge of the injector stream, mixing with ambient air is detected, shown by a decrease in mean signal and an increase in the standard deviation. Note that outside of the injector stream, in the ambient air, the mean signal is very small, and the standard deviation over mean is quite large. This is due to the low scattering cross section of air compared to

the diesel vapor, and the presence of dust particles in the air which produced a large ratio of standard deviation / mean.

The next test that was performed with diesel fuel consisted of varying the injector temperature for fixed diesel flow rates (37 and 48 mg/s) and steam flow rate (200 mg/s). The temperature was varied by changing the electrical power input to the heating tape. Rayleigh scattering is linearly proportional to the number density of the gas/vapor mixture for a fixed diesel concentration in steam. Utilizing the ideal gas law, the number density of the mixture is inversely proportional to absolute temperature. Thus, as the temperature is increased, the scattering signal should decrease. This was observed (see Figure 35). Also, the standard deviation over mean of the laser scattering signal did not change significantly as the temperature was increased (see Figure 36).

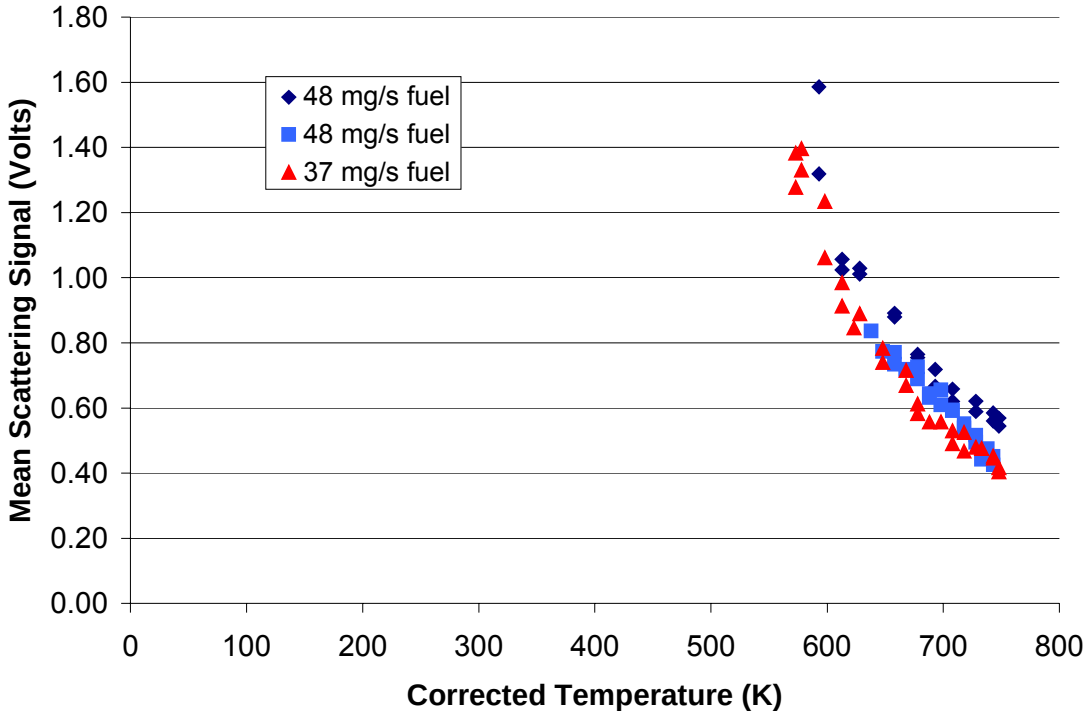

Figure 35: Mean scattering signal plotted versus measured gas temperature at the exit of the injector.

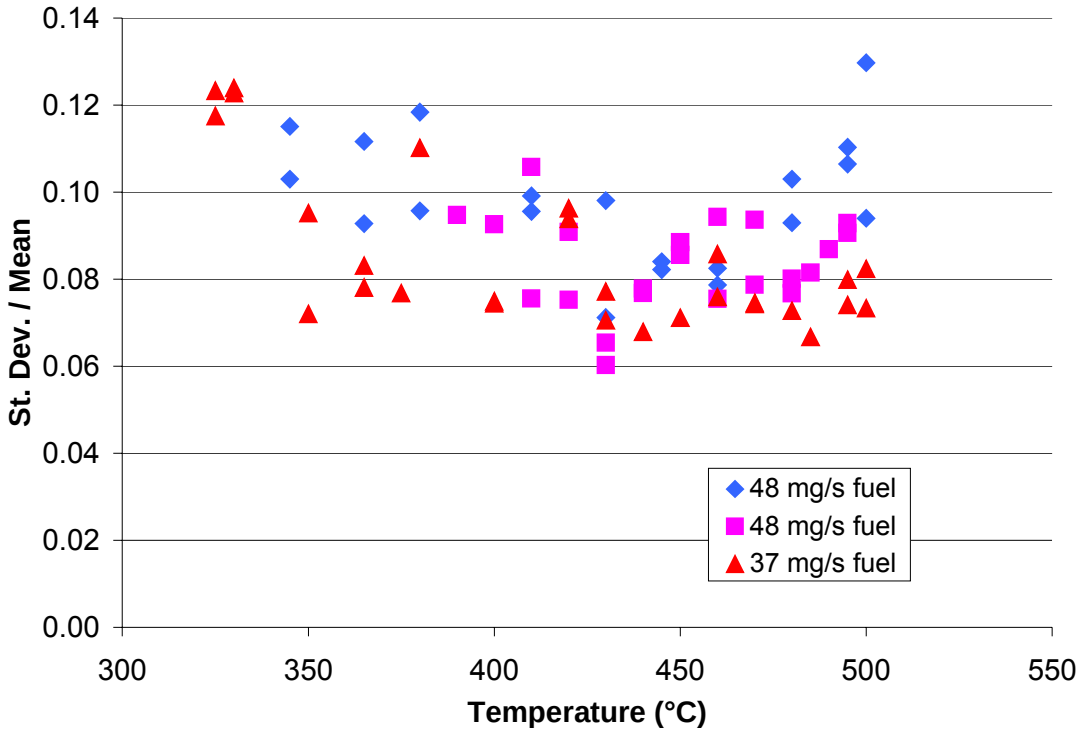

Figure 36: Standard deviation over mean as a function of injector temperature. The temperatures are wall temperatures at the injector exit, the gas temperature is nominally 20 - 30 °C less.

Figure 35 displays the mean scattering signal as a function of injector temperature. A 1/T relationship is expected, but the curve does not mathematically fit this. The decrease is too sharp in slope to agree with 1/T, thus some other process is also affecting the scattering signal. The PM tube was initially tested for linearity and was found to have an R-value of 0.9896 for 8 data points. Thus, it does not appear PM tube non-linearity is a major cause of the greater than expected drop off in scattering signal with increasing temperature. Diesel fuel starts to thermally crack at around 360 °C, thus the temperature results of Figure 35 may indicate cracking of diesel, and consequent lower scattering due to smaller molecules.

Figure 36 implies the mixing is not strongly dependent on temperature. There is a slight minimum in the standard deviation over mean ratio around 450 °C.

InnovaTek injector: Near the conclusion of the testing program, InnovaTek, Inc. personnel made two visits to the UW laboratory. On the first visit, they provided an InnovaTek injector for testing. The InnovaTek injector provided an interesting comparison to the UW injector, since the InnovaTek injector used a 4-fold larger atomizer nozzle area than the UW injector, and thus has a lower steam pressure

drop than the UW injector. Also, the InnovaTek injector did not employ cooling of the liquid fuel feed tube. Thus, upon testing, vapor lock was observed. On the second visit, InnvovaTek personnel provided a version of their injector with a modified diesel feed tube, which reduced the residence time of the fuel in the feed tube. This performed with less vapor lock tendency.

Concluding tests: Concluding tests of the UW injector, conducted during the last week of the experimental program, involved the following experiments:

Long injector tube: Laser Rayleigh scattering measurements for the injector vaporizing tube approximately doubled in length were conducted. These measurements, over the normal range of steam and diesel flow rates, showed essentially the same standard deviation over mean in the scattering signal. That is, lengthening the injector did not significantly improve the mixing of the diesel vapor into the steam. The original length of the vaporizing tube appears to be adequate for the required vaporization and mixing.

High pressure testing, examining for carbon formation: Two 3-hour tests were performed with the injector operated at high pressure (about 75 psig). The steam inlet temperature was 450-500 degrees C, and the injector was maintained at 500 degrees C by using the heating tape. The following was observed:

1. After the 3 hours of running the injector, it was permitted to cool down, and then it was opened up and inspected. No deposits of carbon were seen.

2. On the next day, the test was repeated with a small amount of air bled into the injector with the steam. This was done since there is evidence in the literature (see next section) that the presence of oxygen can promote carbon formation from hydrocarbons. The injector was run for 3 hours, after which its permitted to cool down and then was inspected. No deposits of carbon were seen.

These tests were unable to replicate the small amounts of carbon observed in the early testing of the injector. The cause for this is not known, though possibilities include: 1) different source of diesel fuel used in the final tests, 2) higher temperature of the vaporization tube (500 degrees C versus about 300 degrees C in the early tests), and 3) minor differences in the testing procedure used.

Conclusions

The LRS results show the injector vaporizes the fuel completely – no droplets or carbon aerosols were indicated with the injector operating at design flow rates. Mixing of the diesel vapor into the steam was indicated to be very good. This follows from the low values measured for the ratio of the standard deviation over mean of the scattering signal: 7% in the case of the diesel fuel and about 10% in the case of the naphtha fuel. The value of 7% is very close to ratio measured for

scattering from jets of bottled N_2 and He – thus, the 7% may represent the noise inherent of the laser/optic/electronic system used. The only gross exception was operation under conditions of vapor lock. Vapor lock caused large oscillations in the liquid injection flow rate (sputtering), and thus produced unsteady concentration effects. Vapor lock can be suppressed by cooling the fuel feed tube. The variable temperature data suggest diesel cracking, though this should be studied further. The spatial position tests revealed the mixture is essentially uniform across the injector tube exit. The tests for carbon deposits were inconclusive. Early tests showed small deposit of non-adhering carbon in the injector. The early tests were run at high pressure and used steam of almost 500 degrees C and a vaporizing tube outlet temperature of about 300 degrees. High pressure testing of the injector at the end of the program failed to show carbon formation. These tests were run at about 500 degrees C for both the steam input and vaporizer tube outlet, and included a small amount of air bled into the injector with the steam.

CARBON FORMATION

Literature on carbon formation was reviewed and results were applied to assess the potential for carbon formation in the injector. Gas turbine literature on vaporized premixed lean combustion and chemical process literature on the steam reforming of refinery hydrocarbons were examined. These literature sources discuss the mechanisms of carbon formation, and indicate that carbon formation can be suppressed by maintaining the temperature of the steam-hydrocarbon mixture below about 650 degrees C and by eliminating the leakage of air into the mixture.

Vaporized premixed lean combustion

In the lower temperature range of 400-700 degrees C most of the information is obtained from the gas turbine literature in the context of VPL (vaporized premixed lean) combustion, in which a separate externally-heated fuel vaporizer is used where the liquid fuel is fully vaporized in the absence of combustion air. Next, a static mixing device is used to achieve a homogeneous mixture of vaporized fuel, steam, and combustion air. Various liquid fuels (heating oil, kerosene, gasoline, methanol and ethanol) have been studied at atmospheric pressure. Work on the VPL method is described by Stoffel and Reh (1995), Yang et al. (1997), and Wei et al. (2002). Earlier work on lean-premixed combustion turbines, by the same group, is given by Aigner et al. (1990), Sattelmayer et al. (1990), Döbbeling et al. (1994), and Poeschl et al. (1994).

A typical setup for VPL combustion is shown on Figure 37. With the VPL, liquid fuel is first atomized by superheated steam to a fine spray in a dedicated vaporizer, quickly heated and completely vaporized. This mixture of fuel vapor and steam is mixed with preheated combustion air – a static mixer is used to give a homogeneous mixture. This mixture is then burned in premixed mode at controlled temperature. Superheated steam is employed as the atomizing gas in a two-phase nozzle because such atomizers operate well for highly viscous fuels with a minimal amount of steam over a wide turndown ratio. This approach also increases vaporization rates due to immediate and intensive heat exchange between superheated steam and fuel spray. Adding steam to the fuel lowers the partial vapor pressure and hence the boiling point of the liquid fuel compounds, enabling a complete evaporation of the liquid fuel at a low temperature or high pressure. The presence of steam in the high temperature zone of the vaporizer also suppresses the formation of carbon deposits and may even remove existing carbon deposits, since these may be converted by water to H_2 and CO.

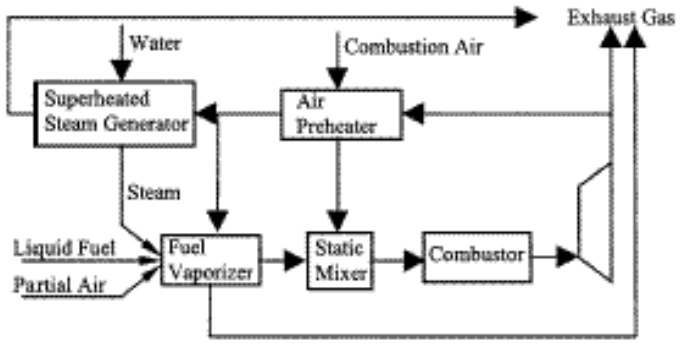

Figure 37: Schematic illustration of the VPL combustion concept (from Wei et al., 2002)

Thermal cracking reactions of hydrocarbons occur in the vaporizer at temperatures higher than 360°C. These endothermic reactions can chemically adsorb extra energy. The cracking reaction yield is determined mainly by temperature and residence time in the vaporizer. Adding a certain amount of air to the vaporizer generates heat through partial oxidation of the fuels, and hence produces a higher temperature in the vaporizer, resulting in faster evaporation. The amount of air added to the vaporizer should not be exceeding 5% of the equivalent combustion air demand.

In experiments by Wei et al. (2002) liquid fuels were atomized with superheated steam through a two-phase nozzle into the free open space of the vaporizer, and were completely vaporized as they passed down through succeeding vertical channels. Air was preheated to temperatures of 400 to 700 degrees C; an electrical heater was employed as the heat source for the vaporizer. The operating pressure was varied between 5 and 30 bar. Although the vaporization time of hexadecane droplets with a size of 50 microns in a hot air stream under conditions in the vaporizer was less than 0.5 ms, the mean residence time of liquid fuels in the vaporizer varied, based on immediate vaporization, from 2 to 10 ms, which is longer than the calculated evaporation time of the droplets. Due to the longer residence time and the temperatures applied, complete evaporation was achieved in the vaporizer.

Cracking or pyrolysis reactions take place when hydrocarbons are exposed to high temperatures. H_2, CO, CO_2 and CH_4 may be found as the products of steam reforming reactions of hydrocarbons at high vaporization temperature, or from oxidation with air. A negligible amount of CO_2 is formed when air is not added to the vaporizer. When air is added, partial oxidation of hydrocarbons occurs and H_2, CO and CO_2 are formed as products of pyrolysis and oxidation. The main reactions in the vaporizer are thermal cracking or pyrolysis, whereby larger hydrocarbons are converted to smaller ones. For No. 2 heating oil, consisting of hydrocarbons from C9 to C27, after vaporization, many small hydrocarbon molecules are formed, and the C16-C27 fraction decreases. Figure 38 shows the

conversion of No. 2 heating oil as a function of average vaporization temperature.

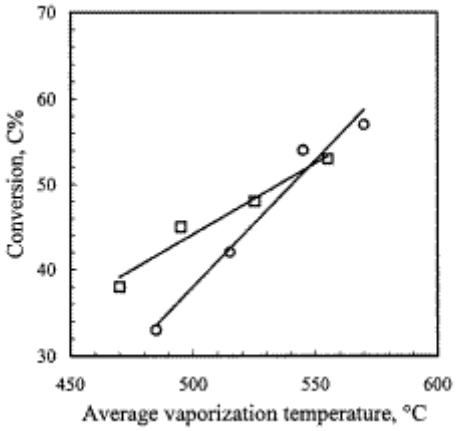

Figure 38: Conversion of No. 2 heating oil during vaporization, as a function of average evaporation temperature (open circles – without additional air to the vaporizer; open squares – with additional air to the vaporizer, 1% of combustion air demand; from Wei et al., 2002)

The conversion increases simply with increasing vaporization temperature. If a small amount of air (1% of the combustion air demand) is added to the vaporizer, conversions at lower vaporization temperatures become higher than in vaporization without air addition. This may be caused by higher temperatures in the initial zone of the vaporizer where the strongly exothermic oxidation reactions occur very fast, providing time at higher temperature for components to be cracked.

The other fuels investigated (kerosene and gasoline) were less reactive. In comparison to the conversion of heating oil, the conversion of the gasoline increased only slightly with increasing vaporization temperature. A significant increase in conversion was observed when a small amount of air was added to the vaporizer.

Adding air to the vaporizer can accelerate the cracking reactions. This is accompanied by the formation of carbon deposits in the vaporizer. In the work reviewed, carbon deposits were found near the nozzle where the fuel first come into contact with air. No carbon deposits were found when air was not added, even at high vaporization temperature (670 degrees C).

Steam reforming

The steam reforming of hydrocarbons is a well-covered area in the literature. The process of steam cracking involves a transfer-line heat exchanger (TLE or TLX). The feedstock coming into the TLE can vary from light hydrocarbons to naphtha and gas-oil types of liquids. The flow comes into the TLE at a temperature of 750-850 degrees C where it is rapidly cooled. The residence time in the TLE up

to the point where the cracking is completed is between 8 and 30 ms. (In the current diesel-steam injector operated at 1 atm pressure, the residence time is about 10 ms). Coke formation and deposition in the TLE are the major reasons in its failure.

In general, there are four known mechanisms for coking, as proposed by various researchers in this field:

- Pyrolytic coke formation.
- Catalytic coke formation.
- Condensation of high boiling components.
- Deposition of mechanically transferred coke in downstream equipment.

In the case of the current diesel-injector injector, any of these mechanisms may be of relevance.

Pyrolytic coke formation: This is also known as radical coke formation. As the nature of the cracking reactions determines, a fractional population of free radicals in the process stream may go through thermodynamically favorable reactions to form coke wherever temperatures are high. Radicals as coke precursors may quickly form pyrolytic coke in the gas phase and deposit non-preferentially on surfaces. This mechanism is observed, for example, in the case of ethane cracking. However, with heavier feedstocks this coking mechanism is considered to be of secondary importance (Lohr et al., 1978).

Lahaye et al. (1977) proposed a mechanism of polymerization of aromatic components towards coke formation. Starting with simple aromatics, multi-ring aromatic components of higher molecular weight form through dehydrogenation/nucleation reactions and then go on to form coke particulates in the gas phase. However, this mechanism is regarded to be relatively unimportant at temperatures below 700 degrees C. Nohara and Sakai (1992) reported that, at temperatures below 600 degrees C, gas-phase reactions at the early stage of coke formation are mainly attributed to a Diels–Alder type reaction. The adhesive fragment-hydrocarbons such as butadiene or the alkyl radical add to unsaturated hydrocarbons to produce C_5 or C_6 cyclic compounds. Thereafter, further cyclo-addition of these fragment-hydrocarbons to cyclic olefins occurs. Polymerization of pure aromatics accompanying dehydrogenation contributes a little to polycyclization. That is, not only ring formation but also growth of the rings proceeds mainly by a Diels–Alder type reaction of butadiene or the alkyl radical, and not by polymerization of pure aromatics below 600 degrees C. From this literature, differences are noted as to the temperature range for this type of polymerization of aromatics to occur.

The pyrolytic coking rate decreases rapidly with decreasing temperature (Froment, 1990). Tesner (1984) summarized the kinetic rates of coke formation from individual hydrocarbons based on his work on coke formation on inert

quartz surfaces as well as others. For comparison, the ratios between the rates at 800 degrees C and the rates at 600 degrees C are given Table 2.

Table 2: Pyrolytic carbon formation rates of hydrocarbon compounds (from Tesner, 1984)

Hydro-carbon	Temperature range (°C)	($g\ cm^{-2}\ s^{-1}\ Pa^{-1}$)		Rate ratio[a] (800/600°C)
		Rate equation [7] (1st order)	Rate at 600°C[a]	
Methane	650–1300	$8.0 \times 10^{-3}\ exp(-272\,000/RT)$	4.27×10^{-19}	1078
Ethane	610–700	$4.9 \times 10^{-3}\ exp(-268\,000/RT)$	4.51×10^{-19}	973
Propane	560–610	$4.6 \times 10^{-3}\ exp(-264\,000/RT)$	7.39×10^{-19}	877
Ethylene	500–700	$7.6 \times 10^{-7}\ exp(-155\,000/RT)$	4.06×10^{-16}	54
Propylene	550–650	$4.0 \times 10^{-7}\ exp(-151\,000/RT)$	3.72×10^{-16}	48
Butadiene	475–600	$7.5 \times 10^{-7}\ exp(-142\,000/RT)$	2.39×10^{-15}	38
Benzene	750–870	$3.0 \times 10^{-3}\ exp(-230\,000/RT)$	5.22×10^{-17}	366
Toluene	650–850	$9.9 \times 10^{-2}\ exp(-243\,000/RT)$	2.87×10^{-16}	512
Xylene	600–750	$1.6 \times 10^{-1}\ exp(-239\,000/RT)$	8.05×10^{-16}	462
Naphthalene	750–850	$6.6 \times 10^{-3}\ exp(-222\,000/RT)$	2.87×10^{-16}	298
Anthracene	730–900	$1.9 \times 10^{-2}\ exp(-218\,000/RT)$	1.73×10^{-15}	269
Acetylene	550–1100	$1.7 \times 10^{-6}\ exp(-138\,000/RT)$	9.43×10^{-15}	35

Table 2 indicates the following:

- The absolute coke formation rates are in the order: acetylene>olefins>aromatics>paraffins. The formation rates of pyrolytic coke from olefins are about 2–4 orders of magnitude higher than from paraffins.
- Within the same group, larger hydrocarbons have highest coke formation rates.
- The temperature dependencies (rate ratio for 800/600 degrees C) are in the order of paraffins>aromatics>olefins>acetylene.

Although the temperatures in the current diesel-steam injector are lower than those reported in the TLE literature, Table 2 suggests that given sufficient residence time, pyrolytic carbon may form. The zones with long residence time can occur when there is a non-ideal flow distribution, such as the recirculation zone behind the injector nozzle block.

Condensation of high boiling components: If the outside of the diesel-steam injector is not insulated, the high boiling hydrocarbons might deposit on the wall and continue to react in the boundary layer and change into high molecular carbon containing substances. This mechanism is most active at the end of the TLE where the wall temperature is the lowest. See Figure 39. As reported in Lohr et al. (1978), this mechanism is a primary coke contributor for heavy feedstocks.

TLX temperature profiles for gas-oil cracking

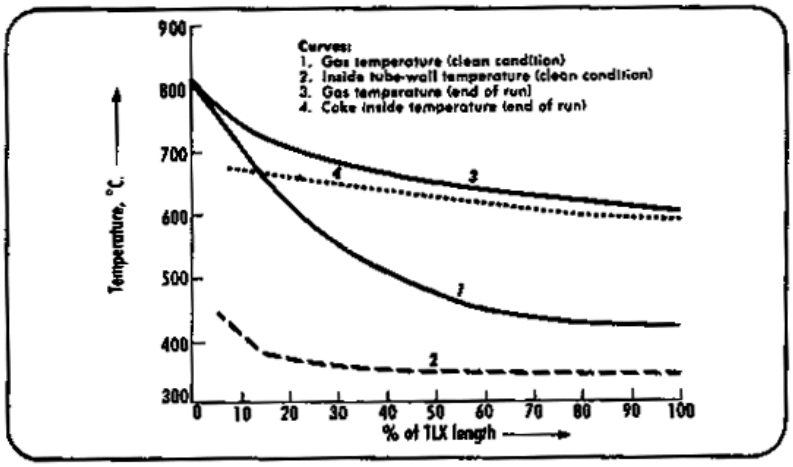

Figure 39: TLE temperature profile (from Lohr et al., 1978).

Table 3 shows the components that are present from the cracking of the liquid feedstock.

Table 3: High-boiling components of liquid feedstock cracking (from Lohr et al., 1978).

Some high-boiling components in effluent gas

Name	Formula	Mol wt	Boiling point °C.	Name	Formula	Mol wt	Boiling point °C.
Naphthalene	$C_{10}H_8$	128	218	Benzo-(m-n-o-) fluoranthene	$C_{18}H_{10}$	226	432
Pentamethylbenzene	$C_{11}H_{16}$	148	230	Tetracene	$C_{18}H_{12}$	228	≈450
Biphenyl	$C_{12}H_{10}$	154	256	Perylene	$C_{20}H_{12}$	252	≈460
Hexamethylbenzene	$C_{12}H_{18}$	162	265	11, 12-Benzofluoranthene	$C_{20}H_{12}$	252	481
Anthracene	$C_{14}H_{10}$	178	340	34-Benzopyrene	$C_{20}H_{12}$	252	496
Phenanthrene	$C_{14}H_{10}$	178	340	1, 2-Benzonaphthacene	$C_{22}H_{14}$	278	≈500
Fluoranthene	$C_{16}H_{10}$	202	383	1, 12-Benzoperylene	$C_{22}H_{12}$	276	≈500
				Picene	$C_{22}H_{12}$	276	≈518
Pyrene	$C_{16}H_{10}$	202	393	1, 2:2', 1' Naphtha-5, 6-benzo-anthracene	$C_{26}H_{14}$	326	≈530

In general, the amount of the high boiling components are the aromaticity of the feedstock are of primary importance in determining the coking rates (Kopinke et al., 1993).

Experiments in laboratory reactor: Kopinke et al. (1993) studied solid deposits that occur at two positions in steam crackers: at the walls of the pyrolysis reactor (coil) and at the walls of the transfer line heat exchanger (TLE). Both types of

deposits, the coil coke and the TLE coke, were studied in a laboratory pyrolysis reactor (Figure 40). The reactor consisted of an electrically heated quartz tube (*l* = 30 cm, *id* = 1 cm). By combination of several heating sections a temperature profile was produced at the reactor exit, so that the coil coke and the deposits in the cooling section (as a rough equivalent of a TLE) could be determined separately. The zone between them, corresponding to a temperature range of 500-700 degrees C, was almost free of deposits.

The nominal pyrolysis conditions of these tests were as follows:

- T_r = 810°C
- residence time = 0.4 s
- total pressure = 0.1 MPa
- dilution ratio steam/naphtha = 0.7 g/g
- ratio of ethene/propene in the cracked gas = 2.5 g/g
- feedstock of straight run naphtha within the boiling range of 50-180°C.

Hydrocarbon feedstocks, diluted with nitrogen or steam, were injected into the top of the reactor. Inside the reactor, “coupon” surfaces of different shape (foils or tubelets of about 3 cm^2 surface area) and material (steels or quartz) were suspended. The thermo-balance permitted a continuous measurement of the coke deposition on a coupon surface in the cracking zone (~800°C) as well as in the post-cracking zone (200-500°C).

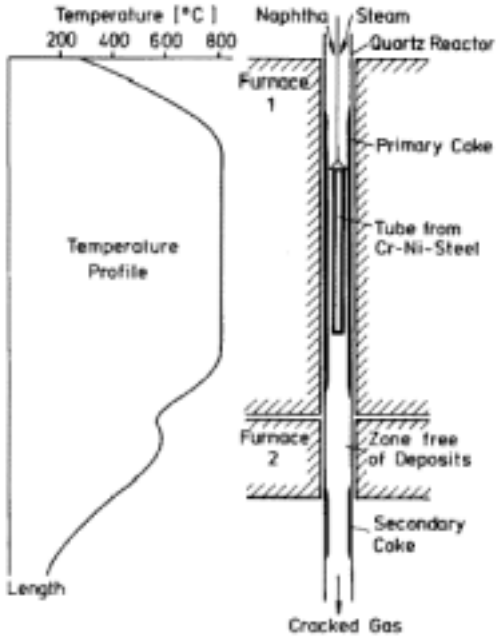

Figure 40: Laboratory pyrolysis reactor for studies of coke formation (from Kopinke et al., 1993)

Figure 41 shows some relative rate constants of selected hydrocarbons. As one might expect, polycyclic aromatics like acenaphthylene, methylanthracene, and chrysene were the most important precursors of deposits. Simple aromatic hydrocarbons such as benzenes or unsubstituted naphthalene were much less important.

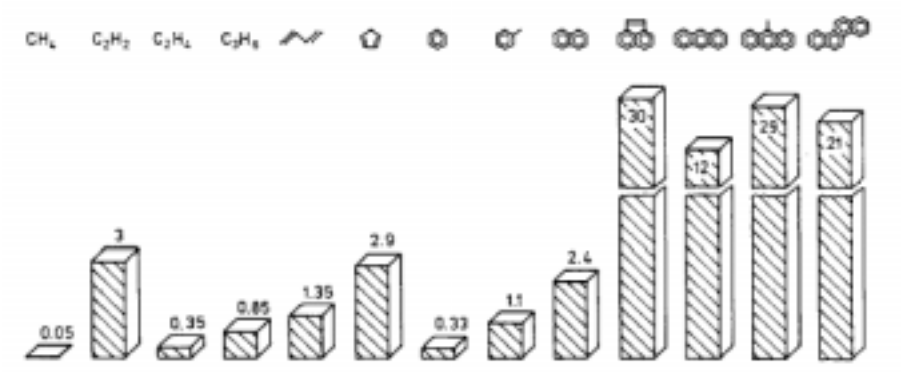

Figure 41: Relative rate constants of TLE fouling of selected hydrocarbons (from Kopinke et al., 1993)

There are questions about which mechanism governs the TLE fouling. The TLE fouling does not appear to be a simple continuation of the high-temperature coil coking at a decreased temperature level. There are at least four plausible alternatives:

(i) Physical condensation of high boiling components of the reactor effluent at the cooled TLE walls.
(ii) Mechanical deposition of tar droplets, which are formed early in the cracking zone.
(iii) Chemical reaction between the growing coke layer and reactive species from the gas phase.
(iv) Chemical reaction as in (iii), but catalyzed by metal particles, well dispersed through the coke matrix.

The temperature dependency of the fouling rate (Figure 42) favors the physical condensation as a key step.

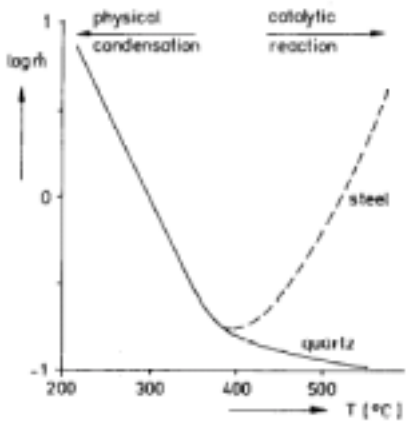

Figure 42: Temperature dependence of the fouling rate [T_a = 800°C, isobutane: N = 2 gmol/gmol] (from Kopinke et al., 1993)

With increasing temperature of the coupon surface, the deposition rate decreases. This is in line with the experience of industrial TLEs: the fouling rate is highest at the end of the TLE where the wall temperature and the gas temperature are the lowest. The curve in Figure 42 also gives evidence of a catalytic contribution to the TLE fouling, if the coupon surface has an active surface, e.g., a low-alloyed steel. Its catalytic activity, however, only becomes significant at temperatures above 400 degrees C. For catalytically inactive materials, such as quartz and high alloyed Cr-Ni-steels, the fouling rate leads to very low values, which correspond to a growth of the coke layer thickness of a few pm per day only.

Steam acts as a catalyst poison in the TLE. The addition of steam to dry cracked gas from isobutane reduces the fouling rate by more than one order of magnitude, down to a low level that is stable over long periods. The portion of added steam amounts to 50 %wt with respect to the hydrocarbon. This is a usual ratio in steam cracking of light feedstocks. After stopping the steam injection the fouling rate rises again. There are three hypotheses to understand the effect of steam on the coking rate:

(i) Gasification of coke.
(ii) Blockage of active centers.
(iii) Oxidation of iron and/or destruction of iron carbides.

The gasification of coke can be ruled out, because in the TLE experiments no CO was observed and the coke covered coupon surface was weight stable in a steam atmosphere free of hydrocarbon. Obviously, 500°C is too low a temperature to start a steam reforming of the coke. If adsorption-desorption steps were determining, then the effects would be expected to follow rapidly after injection and taking off steam. The weight changes, however, follow the changes in steam dilution slowly. The most convincing explanation of the findings

presented in Figure 43 is a reversible oxidation-reduction cycle, in which steam acts as the oxidation agent. This agrees with all the experimental observations, especially the prompt weight changes at the switching points. Consequently, a reduced iron surface has to be considered as active and a partially oxidized surface as inactive in hydrocarbon decomposition.

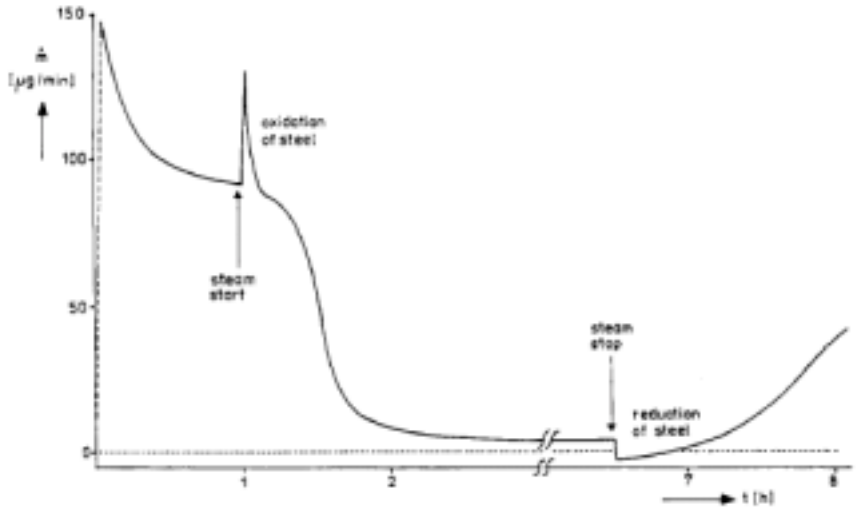

Figure 43: Coke formation on a coupon of 15Mo3 steel at 500°C from cracked isobutane [T_r = 800C, HC: H,O = 2 g/g, HC:N = 2 mol/mol] (from Kopinke et al., 1993).

Conclusions

In the current diesel-steam injector, based on the literature, one might expect:

- Catalytic cracking of fuel taking place at the temperature as low as 350 degrees C.
- Solid deposits forming on the wall at the temperatures of 650 degrees C or higher, without the presence of air in the fuel-steam mixture.
- In the presence of oxygen, carbon deposits forming at the temperatures as low as 450 degrees C.
- The formation of carbon deposits mainly depending on the temperature and residence time in the injector
- Low-alloy steel most likely would be catalyst for forming deposits, though steam in this situation would act as the poison and would decrease the carbon formation.

CONCLUSIONS

The LRS results show the injector vaporizes the fuel completely – no droplets or carbon aerosols were indicated with the injector operating at design flow rates. Mixing of the diesel vapor into the steam was indicated to be very good. This follows from the low values measured for the ratio of the standard deviation over mean of the scattering signal: 7% in the case of the diesel fuel and about 10% in the case of the naphtha fuel. The value of 7% is very close to ratio measured for scattering from jets of bottled N_2 and He – thus, the 7% may represent the noise inherent of the laser/optic/electronic system used. The only gross exception was operation under conditions of vapor lock. Vapor lock caused large oscillations in the liquid injection flow rate (sputtering), and thus produced unsteady concentration effects. Vapor lock can be suppressed by cooling the fuel feed tube. The variable temperature data suggest diesel cracking, though this should be studied further. The spatial position tests revealed the mixture is essentially uniform across the injector tube exit.

The tests for carbon deposits were inconclusive. Early tests showed small deposit of non-adhering carbon in the injector. The early tests were run at high pressure and used steam of almost 500 degrees C and a vaporizing tube outlet temperature of about 300 degrees. High pressure testing of the injector at the end of the program failed to show carbon formation. These tests were run at about 500 degrees C for both the steam input and vaporizer tube outlet, and included a small amount of air bled into the injector with the steam.

The literature reviewed on carbon formation indicates the following:

- Catalytic cracking of fuel taking place at the temperature as low as 350 degrees C.
- Solid deposits forming on the wall at the temperatures of 650 degrees C or higher, without the presence of air in the fuel-steam mixture.
- In the presence of oxygen, carbon deposits forming at the temperatures as low as 450 degrees C.
- The formation of carbon deposits mainly depending on the temperature and residence time in the injector
- Low-alloy steel most likely would be catalyst for forming deposits, though steam in this situation would act as the poison and would decrease the carbon formation.

RECOMMENDATIONS

It is strongly recommended that this work be continued in the following critical areas:

1. Detailed examination of carbon formation in the injector, determining those operating conditions under which carbon formation can be controlled. This could be accomplished in part using a carbon probe to ascertain carbon formation as a function of injector operating conditions. Now that good vaporization and mixing have been demonstrated for the injector, the areas remaining for commercial success of the injector are understanding and preventing carbon deposits in the injector.
2. Examination of cracking reactions in the injector, determining the extent to which new hydrocarbons, hydrogen, and oxides of carbon are formed in the injector. This could be accomplished in part by conducting a series of sample extractions followed by gas chromatographic analysis of the samples.

REFERENCES

M. Aigner, A. Mayer, P. Schiessel, and W. Strittmatter, Second generation low emission combustor for ABB gas turbines: tests under full engine condition, ASME Paper 90-GT-308 (1990).

A. Cavaliere, R. Ragucci, A. D'Alessio, and C. Noviello, "Analysis of diesel sprays through two-dimensional laser light scattering," 22nd International Symposium on Combustion (1988), The Combustion Institute, Pittsburgh, PA, pp. 1973-1981.

K. Döbbeling, K.P. Knoepfel, W. Polike, D. Winkler, C. Steinbach, and T. Sattelmayer, "Low NOx premixed combustion of MBTU fuels using the ABB double cone burner (EV burner)", ASME paper 94-GT-394 (1994).

C. Espey and J. Dec, "Planar laser rayleigh scattering for quantitative vapor-fuel imaging in a diesel jet." *Combustion and Flame* **109** (1997), pp. 65 – 86.

G.F. Froment, Rev. *Chem. Eng.* **6** (1990), p. 293.

W. C. Gardiner, Y. Hidaka, T. Tanzawa, "Refractivity of Combustion Gases," *Combustion and Flame* **40** (1981), pp. 213 – 219.

K. D. Kihm, G. M. Lyn, and S. Y. Son, "Atomization of cross-injecting sprays into convective air stream," *Atomization and Sprays* **5***,* (1995) pp. 417-433.

F. Kopinke, G. Zimmermann, G.C. Reyniers and G.F. Froment, *Ind. Eng. Chem. Res*. **32** (1993), p. 56

J. Lahaye, P. Badie and J. Ducret, *Carbon* **15** (1977), p. 87

J. C. Y. Lee, "Reduction of NOx emission for lean prevaporized-preimxed combustors," Ph.D. Thesis, University of Washington, Seattle (2000).

A. H. Lefebvre, *Atomization and* Sprays, Hemisphere Publishers, New York: Hemisphere (1989).

B. Lohr, H. Dittman and A.G. Linde, *Journal Oil Gas* **76** (1978), pp. 63–68

D. Nohara and T. Sakai, *Ind. Eng. Chem. Res.* **31** (1992), p. 14

G. Poeschl, W. Ruhkamp, and H. Pfost, "Combustion with low pollutant emission of liquid fuels in gas turbines by premixing and prevaporization," AMSE Paper 94-GT-443 (1994).

T. Sattelmeyer, M.P. Felchlin, J. Hellat, and D. Styner, “Second generation low emission combustor for ABB gas turbines, burner development and tests at atmospheric pressure,” ASME Paper 90-GT-162 (1990).

B. Stoffel and L. Reh, “Conversion of liquid to gaseous fuels for lean premixed combustion,” ASME Paper 95-GT-412 (1995).

P.A. Tesner, *Chem. Phys. Carbon* **19** (1984), p. 65

Y. Wang, L. Reh, D. Pennell, D. Winkler, and K. Döbbeling, “Conversion of liquid to gaseous fuels for prevaporized premixed combustion in gas turbines,” ASME Paper 97-GT-225 (1997).

M Wei, Y Wang, and L Reh, “Experimental investigation of the prevaporized premixed (VPL) combustion process for liquid fuel lean combustion,” *Chemical Engineering and Processing*, Volume 41, Issue 2, February 2002, Pages 157-164.

D. Yee, “ExperimentalsStudy of turbulent mixing in nonburning and burning hydrogen-air coaxial jets,” Ph. D. Dissertation (1982), Washington State University, Pullman, WA.